



Quercus ilex L. dieback is genetically determined: Evidence provided by dendrochronology, $\delta^{13}\text{C}$ and SSR genotyping

Francesca Alderotti^{a,b,c,1}, Fabiano Sillo^{b,c,1}, Lorenzo Brilli^d, Filippo Bussotti^a, Mauro Centritto^{b,c}, Francesco Ferrini^{a,b,c,e}, Antonella Gori^{a,b,c}, Roberto Inghes^{b,c}, Dalila Pasquini^a, Martina Pollastrini^{a,e}, Matthias Saurer^f, Paolo Cherubini^{f,g,2}, Raffaella Balestrini^{b,c,2}, Cecilia Brunetti^{a,b,c,*,2}

^a University of Florence, Department of Agriculture, Food, Environment and Forestry, Viale delle idee 30, 50019 Sesto Fiorentino, Piazzale delle Cascine 28, 50144 Florence, Italy

^b National Research Council of Italy (CNR), Institute for Sustainable Plant Protection, Via Madonna del Piano 10, 50019 Sesto Fiorentino (FI), Italy

^c Strada delle Cacce 73, 10135, Torino, Italy

^d CNR-IBE, National Research Council of Italy (CNR), Institute for the BioEconomy, Via Caproni 8, 50145 Firenze, Italy

^e National Biodiversity Future Center (www.nfbc.it), Italy

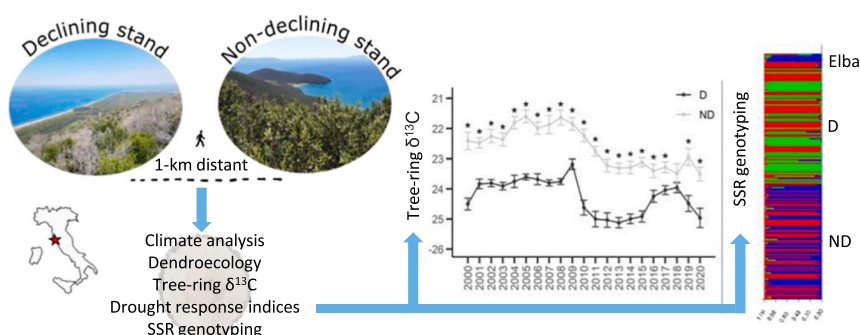
^f WSL Swiss Federal Institute for Forest, Snow and Landscape Research, Zürcherstrasse 111, CH-8903 Birmensdorf, Switzerland

^g University of British Columbia, Department of Forest and Conservation Sciences, Vancouver, BC, Canada

HIGHLIGHTS

- Two close *Q. ilex* stands differing in crown damage levels were studied.
- Dendrochronology, tree-ring $\delta^{13}\text{C}$ and SSR genotyping were applied.
- Genetics showed intraspecific variations in drought response between the two stands.
- The two *Q. ilex* populations differed in water use efficiency (WUE).

GRAPHICAL ABSTRACT



ARTICLE INFO

Editor: Manuel Esteban Lucas-Borja

Keywords:

Dendrochronology
Dieback
Drought stress

ABSTRACT

Quercus ilex L. dieback has been reported in several Mediterranean forests, revealing different degree of crown damages even in close sites, as observed in two *Q. ilex* forest stands in southern Tuscany (IT). In this work, we applied a novel approach combining dendrochronological, tree-ring $\delta^{13}\text{C}$ and genetic analysis to test the hypothesis that different damage levels observed in a declining (D) and non-declining (ND) *Q. ilex* stands are connected to population features linked to distinct response to drought. Furthermore, we investigated the impact

* Corresponding author at: National Research Council of Italy (CNR), Institute for Sustainable Plant Protection, Via Madonna del Piano 10, 50019 Sesto Fiorentino (FI), Italy.

E-mail address: cecilia.brunetti@ipspp.cnr.it (C. Brunetti).

¹ These authors equally contributed to the work as first author.

² These authors equally contributed to the work.

Mediterranean forest
Quercus ilex
 SSR genotyping
 Tree-ring $\delta^{13}\text{C}$
 Water strategy

of two major drought events (2012 and 2017), that occurred in the last fifteen years in central Italy, on *Q. ilex* growth and intrinsic water use efficiency (WUE_i). Overall, *Q. ilex* showed slightly different ring-width patterns between the two stands, suggesting a lower responsiveness to seasonal climatic variations for trees at D stand, while *Q. ilex* at ND stand showed changes in the relationship between climatic parameters and growth across time. The strong divergence in $\delta^{13}\text{C}$ signals between the two stands suggested a more conservative use of water for *Q. ilex* at ND compared to D stand that may be genetically driven. *Q. ilex* at ND resulted more resilient to drought compared to trees at D, probably thanks to its safer water strategy. Genotyping analysis based on simple-sequence repeat (SSR) markers revealed the presence of different *Q. ilex* populations at D and ND stands. Our study shows intraspecific variations in drought response among trees grown in close. In addition, it highlights the potential of combining tree-ring $\delta^{13}\text{C}$ data with SSR genotyping for the selection of seed-bearing genotypes aimed to preserve Mediterranean holm oak ecosystem and improve its forest management.

1. Introduction

Climate change is currently threatening forests in Mediterranean ecosystems (Adams et al., 2017). According to predictions based on climatic models, air temperatures are expected to rise, and drought frequency and severity will increase (IPCC, 2022), particularly in the Mediterranean basin, which is considered a “hotspot” for climate change (Giorgi, 2006). Over the past two decades, the occurrence of extreme climatic events in this region has increased, while temperatures have raised by 1.3 °C since the beginning of the 20th century and are expected to further increase (Hartmann et al., 2013; Mariotti et al., 2015). Such climatic pressures contribute to the spread of vegetation dieback over several Mediterranean forest communities, which have shown typical decline symptoms, such as crown defoliation, leaf desiccation, and production of epicormic shoots (Natalini et al., 2016; Hereş et al., 2018). Worrisomely, dieback affects even tree species considered well adapted to the Mediterranean environmental conditions, such as the evergreen *Quercus ilex* L. (holm oak) (David et al., 2007; Alderotti and Verdiani, 2023).

Quercus ilex has a high ecological and economic value as it is the dominant tree species of the Mediterranean coastal and subcoastal woodlands as well as of the Spanish agrosilvopastoral areas (the so called “dehesa”) (Joffre et al., 1999; González-Rodríguez et al., 2011). *Quercus ilex* is a long-lived semi-ring-porous wood tree species known to be drought-tolerant (Cherubini et al., 2003; Corcuera et al., 2004; Campelo et al., 2010). However, it has recently experienced a remarkable drought-related decline and increase in tree mortality rates (Lloret and Siscart, 2004; Rita et al., 2020; García-Angulo et al., 2020). This decline has worsened over the last 15 years, particularly after severe droughts occurred in 2012 and 2017 (Camarero et al., 2015; Rita et al., 2020; Pollastrini et al., 2019).

Drought-related tree-physiological mechanisms associated with vegetation dieback include hydraulic failure and carbon starvation (McDowell et al., 2008, 2011). Hydraulic failure consists of a loss of xylem functionality due to vessel embolism. Carbon starvation refers to an imbalance between tree carbohydrate demand and supply due to a reduction in carbon uptake induced by drought (Lobo et al., 2018). To date, most field studies on *Q. ilex* have been conducted using rainfall exclusion experiments, which allowed the investigation of long-term physiological, biochemical, and ecological responses of the tree to drought stress (Barbeta et al., 2013; Gavinet et al., 2020; Le Roncé et al., 2021; Limousin et al., 2022). However, further studies are needed to unveil the abiotic and biotic causes inducing the *Q. ilex* decline (Rodríguez-Calcerrada et al., 2017; Gori et al., 2023; Alderotti and Verdiani, 2023). In this context, tree-ring analysis allows the retrieval of past key information regarding dieback onset, even when dieback differently affects coexisting individuals of the same species, as in the so-called patchy dieback phenomena (Camarero et al., 2016; Ripullone et al., 2020).

The measurement of tree-ring width is often used, although it is sometimes criticized as an indicator of tree vitality and forest health (Cherubini et al., 2021), allowing the inference of past tree-growth conditions and responses to climate change (Fonti et al., 2010).

Dendrochronological studies of forest dieback processes have sometimes reported lower growth rates in declining trees than in non-declining trees, even over several years prior to a catastrophic drought event (Hereş and Martínez-Vilalta, 2012; Camarero et al., 2015). In other cases, tree growth reduction occurs with a short advance compared with the onset of declining symptoms (López et al., 2021). Furthermore, tree-ring data can be used to define the species’ resistance, recovery, and resilience capacity to measure the tree’s capacity to maintain or restore a certain growth rate after a drought stress period (Lloret et al., 2011). Another powerful method for assessing physiological processes in trees is tree-ring stable isotope analysis. In particular, the tree-ring stable carbon isotope ratio ($\delta^{13}\text{C}$) is an integrated indicator of tree vitality over time and can be used as a proxy for stomatal conductance and intrinsic water use efficiency (WUE_i , the ratio between leaf-level net CO_2 assimilation rate to stomatal conductance for water vapour) (Shestakova and Martínez-Sancho, 2021). Plants, indeed, generally discriminate against the heavier carbon isotope ^{13}C in favour of ^{12}C during the uptake and incorporation of CO_2 . However, under stress conditions, such as water shortage, when plants reduce leaf stomatal opening, ^{13}C discrimination declines, resulting in tree ring $\delta^{13}\text{C}$ enrichment (Farquhar et al., 1989; McCarroll and Loader, 2004). Thus, tree-ring $\delta^{13}\text{C}$ is one of the most prominent instruments for investigating long-term changes in water and gas exchange dynamics (Farquhar and O’Leary, 1982; Farquhar et al., 1989).

Despite the importance of studying how drought induces forest dieback, only few studies have addressed the association between genetics and drought responses in different forest species (Fernández i Martí et al., 2018; Shamari et al., 2018; Savi et al., 2019; Fasanella et al., 2021). Indeed, genetically based predisposing factors may be crucial in defining the distribution of forest dieback (Voltas et al., 2013; Fasanella et al., 2021). Furthermore, considering the genetic basis of $\delta^{13}\text{C}$, with varying degrees of heritability found in forest species (Marguerit et al., 2014; Bartholomé et al., 2015; Brendel and Epron, 2022), different genetic backgrounds may explain why neighbouring trees subjected to similar climatic conditions differ in vulnerability to drought stress (Lloret and García, 2016; Petrucco et al., 2017; Colangelo et al., 2018). *Quercus ilex* exhibits high variability in drought tolerance traits both within and among forest patches (Gram and Sork, 2001; San-Eufrasio et al., 2020). Additionally, high population variability and polymorphisms have been found in several species of the genus *Quercus*, highlighting their different capability to cope with drought events (Ramírez-Valiente et al., 2009). Therefore, a more accurate identification of the genetic relationships among declining and non-declining trees, especially when they are close, would improve our understanding of the causes of *Q. ilex* dieback.

Because the concept of tree vigour is complex, multiple descriptors of tree vitality must be used when investigating *Q. ilex* dieback in its natural environment (Cherubini et al., 2021). In this context, we studied the recently observed dieback of *Q. ilex* in southern Tuscany (Italy) in two stands 1 km apart characterized by different crown-dieback levels. We hypothesized that declining (D) and non-declining (ND) trees differ in their ability to cope with drought. We expected: i) growth decline in D trees as an early warning of crown dieback; ii) differences in tree-ring

$\delta^{13}\text{C}$ signals between D and ND trees; and iii) differences in the genetic background that could differentiate the susceptibility of the two stands to drought-induced mortality.

2. Materials and methods

2.1. Study area

The study area is located in the Maremma Regional Park, located on the coast of southern Tuscany (Italy, Fig. 1A), and is characterized by a typical Mediterranean climate, with warm and dry summers and mild winters. The vegetation of the area is the Mediterranean maquis, mainly dominated by *Q. ilex* and understory evergreen vegetation, such as *Erica arborea* L., *Arbutus unedo* L., *Phillyrea* spp., *Pistacia lentiscus* L. and *Myrtus communis* L. *quercus ilex* stands grow at the two selected sites, each of 450 m² (Fig. 1B, C), located 1 km apart. A more detailed description of the vegetation composition and soil texture at both sites can be found in the study by Pasquini et al. (2023). Such stands were managed as coppices until the early eighties in the past century and are now abandoned and characterized by different amounts of *Q. ilex* crown dieback. At the first site approximately 80 % of the dominant trees were in decline, while at the second site, approximately 20 % of the trees showed symptoms of decline (i.e., crown defoliation, leaf desiccation, and abundant dead branches or shoots). Thus, the first site was defined as declining (D) (42°38'22.60" 'N, 11°05'16.04" 'E) and the second site was defined as non-declining (ND) (42°38'04.93" 'N, 11°05'43.24" 'E). In average, basal area at breast height was 60.02 ± 5.55 m²/ha at D site and 53.90 ± 10.9 m²/ha at ND site (Table S1). To describe soil properties, six soil samples were collected in an x-shaped within three plots per site (10 × 15 m²), at a depth of about 40 cm. Different soil samples were combined to obtain a homogeneous sample of approximately 1 kg per plot. The soils at both sites belong to the loam textural class and are characterized by rocky outcrops and neutral pH values (i.e., ~6.5) (i.e., ~6.5) (Table S1). In the study area, *Q. ilex* trees showed no symptoms of decline associated with pathogens (no damage to leaf lamina, no chlorosis, no sunken cankers on branches, trunks, and collars, and no damage in wood tissue) (Linaldeddu et al., 2014).

2.2. Meteorological data and climate analysis

Climate assessment of the study area was performed for the period 1981–2020 using meteorological data collected from the ERA5 database (<https://www.ecmwf.int/en/forecasts/datasets/reanalysis-datasets/era5>) due to the lack of meteorological data for the considered period. Meteorological data included high-resolution (1-h) continuous data of precipitation (PP), mean (T_{mean}), maximum (T_{max}), and minimum (T_{min}) temperatures and net radiance (Rad_n), for a 30 km grid. The selected meteorological variables were grouped into different intervals (daily, monthly, and yearly). The seasonal patterns were first considered as winter (January–March), spring (April–June), summer (July–September), and autumn (October–December). Furthermore, multi-year intervals (1981–1995, 1996–2004, and 2005–2020) were created to consider long-term climate change over the study area based on the most significant changes in meteorological patterns (Ferrio et al., 2021) (Table S2). Precipitation (PP) increased from approximately 380 mm (1981–1995) to 535 mm (in the period 2005–2020). Such increase was more pronounced during winter and autumn. Air temperatures were found to increase from 1981–1995 to 2005–2020 (+0.6 °C for T_{mean} , T_{max} , and + 0.8 °C for T_{min}). Annual Rad_n slightly increased from 1981–1995 to 1996–2004 and then remained stable until 2005–2020 (Table S2).

Drought years were identified using the Standardized Precipitation-Evapotranspiration Index (SPEI). The annual mean of the 12-months SPEI (SPEI12) values from January to December were used to identify drought years over the period 1981–2020 by applying the R Package “SPEI” (Vicente-Serrano et al., 2010) (Table S3).

Meteorological data were employed to calculate the number of months with negative water balance (n. months CWB < 0) and the number of days with daily mean of T_{max} higher than 30 °C (n. days $T_{\text{max}} > 30$ °C). Further, following the approach described in Gazol and Camarero (2022), vapour pressure deficit (VPD) was calculated as the difference between saturation vapour pressure (SVP) and actual vapour pressure (AVP) (Park Williams et al., 2013). Actual vapour pressure monthly data were obtained from database v. 4.05 (<https://crudata.uea.ac.uk/cru/data/hrq/>) (Harris et al., 2020), while SVP was obtained



Fig. 1. (A) Images of the study area with the position of the declining (D, red point) and non-declining (ND, yellow point) sites located in the Maremma Regional Park (Alberese, Grosseto, Italy). Details of *Q. ilex* crowns at the D (B) and ND sites (C).

applying the formula described in (Park Williams et al., 2013) (Eq. (1)):

$$SVP = a_0 + T(a_1 + T(a_2 + T(a_3 + T(a_4 + T(a_5 + T(a_6)))))) \quad (1)$$

where T was mean monthly air temperature expressed in $^{\circ}\text{C}$, $a_0 = 6.1078$, $a_1 = 4.4365 \times 10^{-1}$, $a_2 = 1.4289 \times 10^{-2}$, $a_3 = 2.6506 \times 10^{-4}$, $a_4 = 3.0312 \times 10^{-6}$, $a_5 = 2.0341 \times 10^{-8}$, and $a_6 = 6.1368 \times 10^{-11}$. Monthly VPD data were normalized and grouped to highlight annual and seasonal patterns as described for the others meteorological variables.

2.3. Dendrochronological analyses

Due to the lack of single-stem trees in the study area, five multi-stem *Q. ilex* stumps were selected per site. The dominant trunk of each of the selected stumps was felled, and one cross section per stem at breast height was collected. A detailed description of the trees felled to conduct the study is available in Table S4. Before this field campaign, a small number of woody cores were collected by an increment corer. However, after the preparation of the cores, it was impossible to obtain accurate ring counts on such material due to the weak seasonality of the species and the pronounced parenchyma rays which interfered with the rings lecture. For these reasons, the core samples were discarded, and stem cross section employed (Nijland et al., 2011). Despite the limited number of felled trees due to the Integral Natural Reserve regulations of the Maremma Regional Natural Park, the expressed population signals (EPS) for both D (0.86) and ND (0.83) chronologies were considered satisfactory for the purpose of the study (Wigley et al., 1984; Buras, 2017). The collected samples were air-dried and polished with progressively finer sandpaper (50–400 grit size) to make the rings visible. The ring borders were identified by comparing images found in the scientific literature (Campelo et al., 2010; Zalloni et al., 2018), given the difficulty in dating the tree rings of Mediterranean evergreen species (Cherubini et al., 2003). Furthermore, the intra-annual variation in $\delta^{13}\text{C}$ values along a sample ray was determined using a laser ablation method (described below), improving the validation of the ring-width measurements (Helle & Schleser, 2004b).

Once the samples were dry, tree-ring widths were measured along two radii on each cross section. Measurements to the nearest 0.01 mm were performed with an incremental measuring table (LINTAB, Frank Rinn S.A., Heidelberg, Germany) in combination with the TSAP-Win software (Rinn, 2016) and a Leica MS5 light microscope (Leica Microsystems, Germany). The tree-ring series was first visually cross-dated and successively validated using a statistical procedure implemented in TSAP-Win (*Gleichläufigkeit* values and Student's *t*-test at a significance level of $p < 0.05$). The ring-width series were then converted into ring-width indices (RWI) by fitting a negative exponential curve to remove the effects of tree size and age. The entire detrending process, chronology building, and EPS calculations were performed in R using the dplR package (Bunn et al., 2021).

2.4. Carbon isotopes

Tree-ring $\delta^{13}\text{C}$ was used as a proxy for stomatal regulation and water-use efficiency to examine potential differences in *Q. ilex* at the D and ND sites. For Mediterranean trees, where annual boundaries are sometimes not clear, tree-ring dating and sample preparation for tree-ring $\delta^{13}\text{C}$ analyses can be difficult; however, laser ablation coupled with mass spectrometry is useful for studying the effects of environmental conditions on gas exchange processes with easy sample preparation (Battipaglia et al., 2014).

The $\delta^{13}\text{C}$ -values were determined using a laser ablation-combustion line. The system consist of a sample chamber on a computer-controlled movable 3D-table (isoScell, Terra Analytic, Alba Iulia, Romania), a UV-laser of wavelength 213 nm (Nd:YAG Laser, Teledyne LSX-213 G2+) for ablating the wood spots, a combustion oven, a Cryoflex trace gas

system (Sercon, Crewe, UK) for collection of produced CO_2 and an isotope-ratio mass-spectrometer to measure $\delta^{13}\text{C}$ (HS2022, Sercon, Crewe, UK) (Saurer et al., 2022). $\delta^{13}\text{C}$ -values were measured from 2000 to 2020 on four stem cross section per site, the laser spot size was 100 μm , and the distance between the laser shots was between 300 μm and 550 μm , adjusted to obtain 100 shots and $\delta^{13}\text{C}$ analyses for each tree for the 2000–20 period. A factor of correction was applied to raw $\delta^{13}\text{C}$ data to consider changes in $\delta^{13}\text{C}$ of atmospheric CO_2 and to normalize the data to the year 2000 based on the data sets of Mauna Loa Observatory (Hawaii, https://scrippsco2.ucsd.edu/data/atmospheric_co2/ml0.html). For each year, the mean $\delta^{13}\text{C}$ value was calculated to build an annual $\delta^{13}\text{C}$ -chronology of *Q. ilex* at the D and ND sites.

2.5. Drought response indices

The influence of dry conditions on *Q. ilex* stem growth was assessed using three components of the resilience indices calculated for D and ND trees according to Lloret et al. (2011). Two drought years (2012 and 2017) were considered in the calculation of these indices. This approach was chosen to avoid the lagging effect of the associated drought events between years (Anderegg et al., 2015). A three-year period was chosen as a reference to describe tree growth and stomatal regulation before and after the drought years (Gazol et al., 2017). The stem growth resistance (R_t ; Eq. (2)), recovery (R_c ; Eq. (3)), and resilience (R_s ; Eq. (4)) were calculated using the following equation:

$$R_t = (\text{TRW}_t) / (\text{TRW}_{t-3}) \quad (2)$$

$$R_c = (\text{TRW}_{t+3}) / (\text{TRW}_t) \quad (3)$$

$$R_s = (\text{TRW}_{t+3}) / (\text{TRW}_{t-3}) \quad (4)$$

where TRW_t is the tree-ring width in the target year of the drought event (2012 and 2017), and TRW_{t-3} and TRW_{t+3} were calculated as the mean value of the tree-ring width mean of the three years before and after the drought event, respectively.

R_t quantifies the impact of drought on tree growth compared with the pre-drought period, whereas R_c describes the growth reaction in the years after drought stress. Finally, R_s compares the pre-drought growth with the post-drought growth.

To investigate the effect of drought on *Q. ilex* physiological performances and stress tolerance, the equations of the indices were adapted to $\delta^{13}\text{C}$ values by applying differences rather than ratios, as previously reported by Weigt et al. (2015). Therefore, *Q. ilex* physiological resistance, R_t ($\delta^{13}\text{C}$) (Eq. (5)), recovery, R_c ($\delta^{13}\text{C}$) (Eq. (6)) and resilience, R_s ($\delta^{13}\text{C}$) (Eq. (7)) were calculated using the following equations:

$$R_t (\delta^{13}\text{C}) = (\delta^{13}\text{C}_t - 3) - (\delta^{13}\text{C}_t) \quad (5)$$

$$R_c (\delta^{13}\text{C}) = (\delta^{13}\text{C}_t) - (\delta^{13}\text{C}_{t+3}) \quad (6)$$

$$R_s (\delta^{13}\text{C}) = (\delta^{13}\text{C}_t - 3) - (\delta^{13}\text{C}_{t+3}) \quad (7)$$

where $\delta^{13}\text{C}_t$ is the mean $\delta^{13}\text{C}$ value of the drought year (2012 and 2017), and $\delta^{13}\text{C}_{t-3}$ and $\delta^{13}\text{C}_{t+3}$ were calculated as the $\delta^{13}\text{C}$ mean of the three years before and after the drought event, respectively.

2.6. Genotyping

2.6.1. Sampling and DNA extraction

To assess the genetic background of *Q. ilex* individuals in the D and ND sites, the genotyping of a population of trees was performed. Fresh leaves were collected both from *Q. ilex* trees with and without symptoms of decline and included the trees employed in dendrochronological and tree-ring $\delta^{13}\text{C}$ analysis. All the *Q. ilex* trees available in the three plots per site used for soil sampling analyses, were sampled for genotyping

purpose. Further, a small group of *Q. ilex* trees located on Elba Island (42°47'00.51" N, 10°23'33.90" E) was included in the analyses and used as an outgroup. The sampling campaigns were conducted in 2019 and 2020. In total, fresh leaves were collected from 89 trees showing declining symptoms at the D site, from 90 trees without symptoms at the ND site, and from 11 healthy *Q. ilex* individuals on Elba Island. Samples were 190 in total and were divided as follows: group 1 (plants with symptoms at site D – 90), group 2 (plants without symptoms at site ND – 89), and group 3 (plants from Elba Island – 11). Total DNA was extracted from fresh leaves using a DNeasy Plant Pro Kit (QIAGEN). Quantification and quality assessment of the extracted DNA were performed using a spectrophotometer (NanoDrop 2000, Thermo Scientific™).

2.6.2. SSR genotyping

Two chloroplast (cpSSR) and seven nuclear (nuSSR) simple sequence repeat (SSR) (or microsatellite) loci previously developed on *Quercus robur* and *Quercus petraea* were used for genotyping purposes (Table S5) (Fluch et al., 1997; Deguilloux et al., 2004; Guichoux et al., 2011). In addition, SSR mining of the *Q. ilex* transcriptome, performed using the MSDB software (Microsatellite Search and Building Database) (Du et al., 2013), allowed the identification of perfect trinucleotide SSR in the available transcriptomic sequences of this tree species (Madritsch et al., 2019). Subsequently, perfect trinucleotide SSRs present in five transcript sequences putatively related to plant responses to drought stress (Madritsch et al., 2019) were selected as SSR markers. To assess the presence of introns, sequences were aligned with those of the *Q. rubra* genome harbored by the Phytozome IT platform (Goodstein et al., 2012), and six primer pairs were designed using Primer3Plus (Table S5). Primer pairs were tested using high-resolution melting (HRM) analysis for genotyping 190 sampled individuals. This technique, coupled with SSRs, has proven to be useful and accurate for genotyping several organisms (Sillo et al., 2017), including trees (Gomes et al., 2018). The qPCR for HRM analysis was carried out using the Connect Real-Time PCR Detection System (Bio-Rad). DNA from the samples was diluted to a concentration of 20 ng/μl per sample. Reactions were performed in a total volume of 10 μL, 1 μL of DNA, 5 μL SsoAdvanced Universal SYBR Green Supermix (Bio-Rad) and 0.09 μM each primer, using a 96-well plate. The following PCR protocol, including the calculation of a melting curve, was used: 98 °C for 2 min; 45 cycles of 98 °C for 5 s, 60 °C for 10 s, ramp from 65 to 95 °C with a temperature increment of 0.1 °C per cycle, and a read plate every 10 s. Melting curves were analysed by using PRECISION MELT ANALYSIS software (Bio-Rad), with parameter the “Tm difference threshold” set as 0.10 and the “Melt curve shape sensitivity” as 50. The software grouped the melting curves into clusters representing different alleles of the analysed SSR loci. Alleles were assigned to all samples for each locus and a matrix including all allelic data was prepared (Table S6). A genotype accumulation curve was generated using the R poppr package (Kamvar et al., 2014) to estimate the number of loci required for genotyping all the samples. The data matrix was analysed using GENALEX v. 6.5 (Peakall and Smouse, 2012). The total unbiased allele diversity (uh) per locus and pairwise population matrix of Nei's genetic identity (I) were determined. Bayesian analysis, as implemented by the software STRUCTURE V.2.3.4 (Pritchard et al., 2000), was used to assign individuals to subpopulations. Successive K values (number of populations) from 1 to 10 were used to obtain distinct clusters and estimate the number of subpopulations. Twenty runs each for K = 1 to 10 with 750,000 Markov chain Monte Carlo repetitions after a burn-in period of 500,000 repetitions were performed with the ‘Admixture model’ option and without any prior information on the origin of individual samples. ΔK was determined based on the highest likelihood of the data (LnP(D)) and was used to infer the K value best representing the observed data under the implemented model by using Structure Harvester Web v0.6.94 (Earl and VonHoldt, 2012).

2.7. Statistical analyses

The data were analysed for normality of the distribution and equality of variance, and when at least one of these two assumptions was missing, a non-parametric statistical test was performed.

Non-parametric Mann–Kendall test was applied to estimate any significant long-term trends in the annual number of months with negative CWB, annual number of days with T_{max} higher than 30 °C, annual and seasonal VPD. The significant difference in ring-width indices chronologies (RWI) and $\delta^{13}C$ -chronologies between D and ND was checked using Mann–Whitney U tests ($p \leq 0.05$). Spearman's correlations between *Q. ilex* RWI at D and ND site and annual and seasonal climatic parameters were also performed, as well as RWI correlation with previous annual and autumn climatic parameters. Since the SPEI analysis identified two periods with different water availability, the correlation was tested separately for the years 1998–2004 and 2005–2020. Spearman's correlation was also applied between D and ND $\delta^{13}C$ -chronologies and climatic parameters for the entire of $\delta^{13}C$ data available (2000–2020). Two-way ANOVA followed by Tukey's post-hoc test was applied to analyse the growth patterns and stomatal responses of D and ND *Q. ilex* in 2012 and 2017. All statistical analyses were performed using R, version 4.0.3.

3. Results

3.1. Climate analysis

The SPEI analysis indicated several consecutive drought years in period from 1981 to 1995 (Fig. 2), and occasionally drought years for the remaining years considered in study (Fig. 2). No significant trend was observed for the number of months with negative CWB at the study area (Fig. 3). On the other hand, the number of days with T_{max} higher than 30 °C showed a significant increment over the studied period (Fig. 3). This parameter showed its maximum in 2003, however, also others important peaks were reported in 2006, 2012, 2013, 2015, 2017 and 2019 (Fig. 3). Annual, spring and summer VPD values significantly raised in the study area (Fig. S1A; Fig. 4A, B), while significant modification in winter and autumn VPD values were not observed (Fig. S1B, 1C).

3.2. Dendrochronological analysis and relationships between growth and climatic data

Dendrochronological analysis indicated that *Q. ilex* at D and ND sites showed slightly different ring-width patterns. The ring-width indices (RWI) chronologies at the ND than at the D sites showed a similar pattern during the period 1988–2015 and started to diverge from 2016 (Fig. 5). Significantly differences between the two chronologies were observed in six of the 33 years (Table S7), with higher growth rate values at D compared to ND stand 1995 and 2015, and lower growth rate values at D than ND in 2002, 2005, 2017 and 2019 (Fig. 5).

From 1988 to 2004, RWI at ND site positively correlated with spring precipitation and negatively correlated with annual net radiation (Rad_n) (Table S8A), while no correlation was found at the D site (Table S8A). After 2005, RWI at the ND site positively correlated with the spring mean maximum temperature (T_{max}), annual, and spring net radiation (Rad_n) (Table S8B). Furthermore, negative correlations were found between RWI at ND sites and annual, spring, summer, and autumn SPEI12 (Table S8B). No correlation between RWI at the D site and climate data were found considering the time window 2005–2020 (Table S7B). Finally, RWI did not correlate with previous annual and autumn parameters, either at the D or ND sites, considering both the period 1988–2004 and 2005–2020 (data not shown).

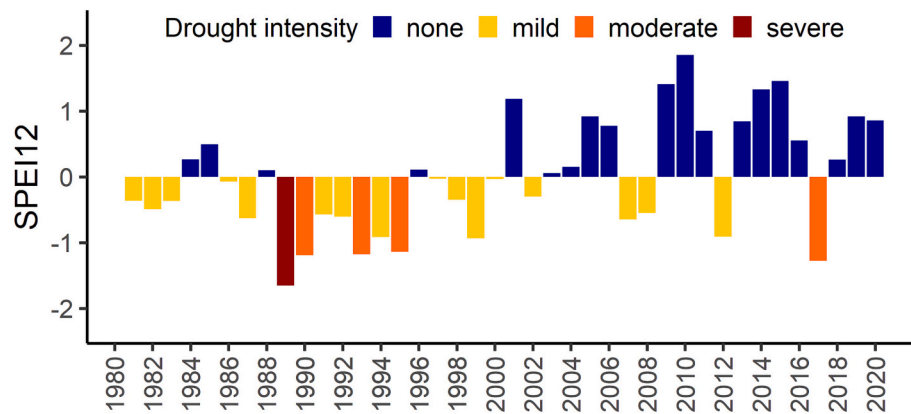


Fig. 2. Annual mean 12-months SPEI values (SPEI12) from 1981 to 2020 for the Regional Natural Park of Maremma (Alberese, Grosseto, Italy). Coloured bars indicate drought intensity.

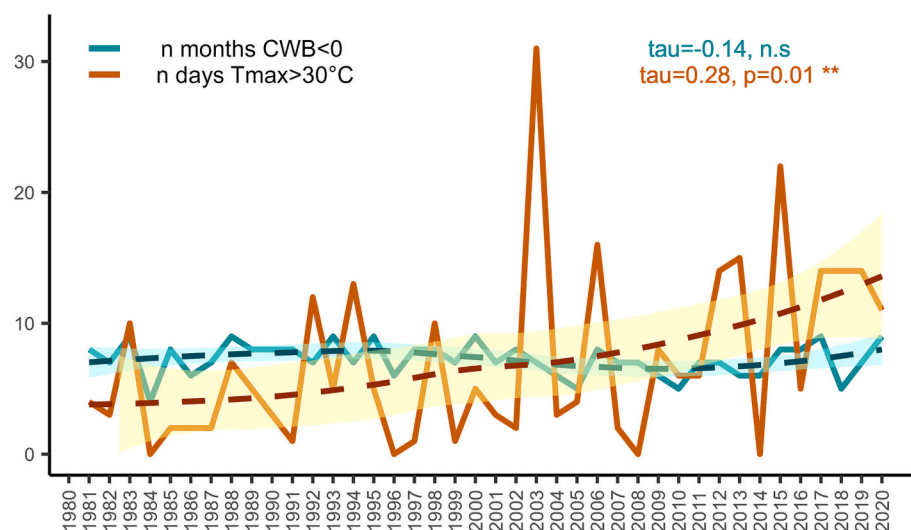


Fig. 3. Annual number of days with $T_{\max} > 30^{\circ}\text{C}$ and annual number of months with negative CWB from 1981 to 2020 for the Regional Natural Park of Maremma (Alberese, Grosseto, Italy). The Mann–Kendall test was applied to estimate significance of long-term trends ($p < 0.05$). Shades represent 90 % confidence intervals.

3.3. Carbon isotopes and climate relationship

A strong divergence in $\delta^{13}\text{C}$ signals emerged between *Q. ilex* at the D and ND sites during the period 2000–2020, where the $\delta^{13}\text{C}$ signal was significantly higher at the ND site than at the D site, except for 2018 (Fig. 6) (Table S9). The $\delta^{13}\text{C}$ -chronologies in *Q. ilex* at the D and ND sites showed a similar trend, with relatively high values at the beginning of the analysed period and a clear decline over the period 2008–2011. The maximum and minimum $\delta^{13}\text{C}$ values were found in 2009 (-23.18 ± 0.65) and 2013 (-25.12 ± 0.85) at D site, and in 2005 (-21.60 ± 0.95) and 2020 (-23.51 ± 1.07) at ND site (Fig. 6).

No significant relationships were found between $\delta^{13}\text{C}$ values and climate variables at site D, whereas $\delta^{13}\text{C}$ was significantly correlated with air temperature parameters at the ND site (Table S10). Specifically, $\delta^{13}\text{C}$ was negatively correlated with the annual and summer T_{mean} ; annual, summer and autumn T_{max} ; annual and winter T_{min} (Table S10).

3.4. Drought response indices

Drought response indices revealed different growth and stomatal responses to the drought events of 2012 and 2017 for *Q. ilex* at D and ND sites. Although *Q. ilex* at D and ND sites showed similar resistance (R_t) to drought in 2012, R_t was reduced at D site compared to ND one in 2017 (-58%). (Fig. 7A). Radial growth recovery capacity (R_c) did not differ

between the D and ND sites in 2012; in contrast, R_c was slightly higher at the D site than at the ND site in 2017 ($+36\%$) (Fig. 7B). Resilience (R_s) levelled off at the ND site, while it significantly reduced at site D from 2012 to 2017 (Fig. 7C), leading to a significant difference between D and ND in 2017 (Fig. 7C).

Furthermore, despite the lack of differences in $R_t(\delta^{13}\text{C})$ between *Q. ilex* at D and ND in the years investigated, $R_t(\delta^{13}\text{C})$ was significantly reduced at site D from 2012 to 2017 (Fig. 7D). $R_c(\delta^{13}\text{C})$ did not vary considering the drought years and the two sites (Fig. 7E). $R_s(\delta^{13}\text{C})$ did not differ between D and ND site, however, $R_s(\delta^{13}\text{C})$ was significantly lower in 2017 than 2012 in both the sites (Fig. 7F).

3.5. Genotyping

The use of 11 SSR loci for genotyping allowed for the generation of a distinct genotypic profile for each sample. The genotype accumulation curves reached a plateau, confirming that the use of 11 markers was sufficient for complete genotyping (Fig. 8A). The overall mean number of detected alleles per locus was 10.91 (ranging from 4 to 23 observed alleles; the number of effective alleles, N_e , from 1238 to 8336), and the overall unbiased Nei's gene diversity (u_h) per locus ranged from 0.183 to 0.885, with an average value of $0.683 (\pm 0.069)$ (Table S10). PCoA on a pairwise matrix of Nei's genetic identity showed two distinct groups, one mainly comprising individuals from the D site, and the other

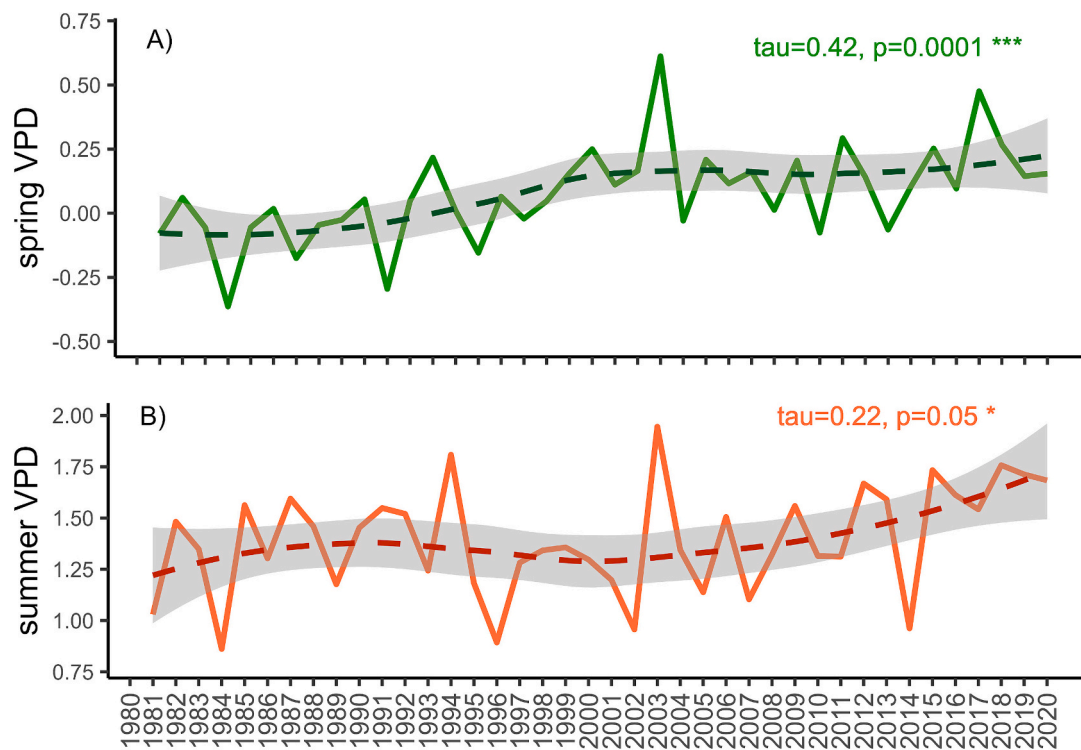


Fig. 4. Seasonal Vapour Pressure Deficit (VPD): spring (A) and summer VPD (B) from 1980 to 2020 for the Regional Natural Park of Maremma (Alberese, Grosseto, Italy). The Mann–Kendall test was applied to estimate significance of long-term trends ($p < 0.05$). Shades represent 90 % confidence intervals.

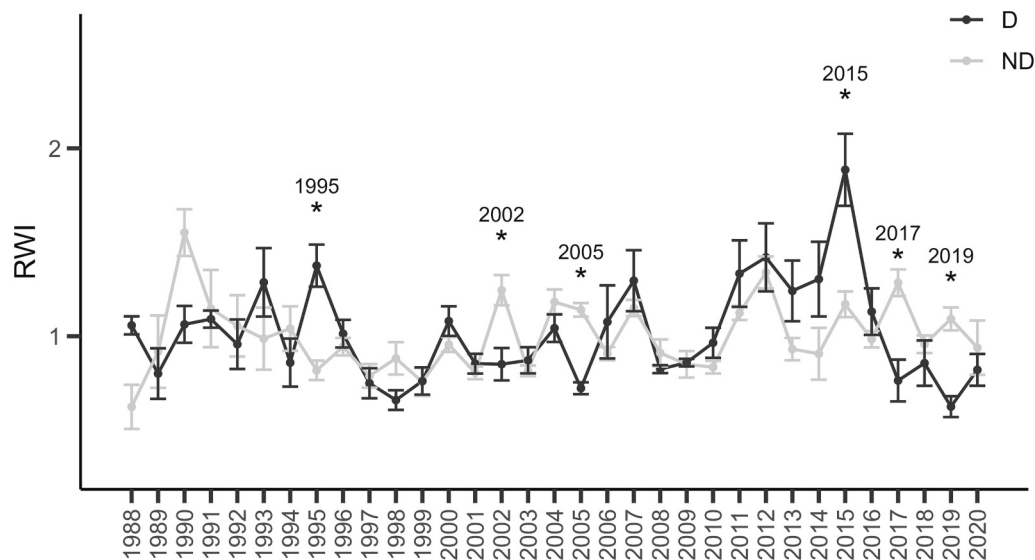


Fig. 5. Tree-ring width indices chronology of *Q. ilex* trees at declining (D) and non-declining (ND) sites. Bars indicate standard errors. The Mann–Whitney *U* test was performed to compare D and ND growth patterns ($n = 5$). Asterisks represent significant differences between the two chronologies ($p < 0.05$).

including individuals from the ND site (Fig. 8B). Samples from Elba Island were clustered between the two groups, with a few exceptions (Fig. 8B). The first two axes of the PCoA explained 22.94 % of the variability, suggesting close relationships within the samples. No significant correlation was detected between pairwise genetic distance and geographical distance among sites (Mantel test between geographical

and genetic distance matrices; $p > 0.05$). Based on the STRUCTURE analysis, the optimal number of populations (K), as inferred by evaluating ΔK , was three (Fig. 8C). Trees from the ND site comprised individuals from two populations as well as trees from Elba Island. Trees from site D were assigned to two populations, one also detected at the ND and Elba sites, and one detected at the D site only (Fig. 8C).

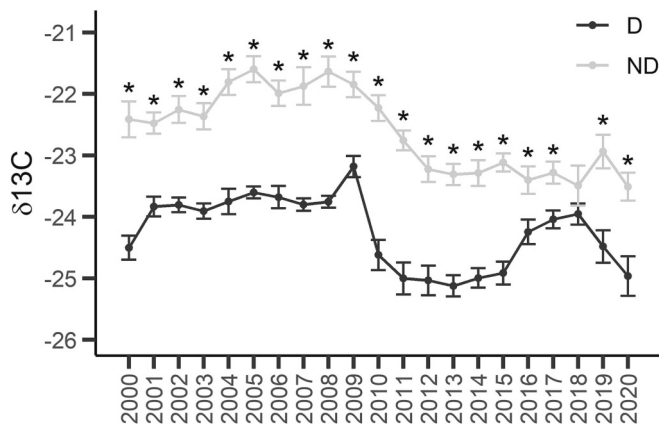


Fig. 6. $\delta^{13}\text{C}$ -chronologies of *Q. ilex* trees at declining (D) and non-declining (ND) sites. Bars indicate standard errors. The Mann-Whitney U test was performed to compare the growth patterns of trees at the D and ND sites ($n = 4$). Asterisks represent significant differences between the two chronologies ($p < 0.05$).

4. Discussion

4.1. Relationship of tree-ring growth and $\delta^{13}\text{C}$ with climate

The SPEI analysis revealed a long and intense dry period from 1980 to 2004 and several dry years after 2005 in the study area. Previous investigations have highlighted that the dry period from 1980 to 2000 was concomitant with *Q. ilex* dieback and a reduction in its growth rates in Spain and Italy (Peñuelas et al., 2000; Lloret and Siscart, 2004; Gentilesca et al., 2017).

Accordingly, our study revealed significantly lower growth rates in trees at the D site compared to those at the ND site, especially in the years immediately after the dry period of 1980–2000 and after 2016

(Fig. 5). The steep increase in vapour pressure deficit (VPD) observed in the study area suggest that the drought period before 2004 was mainly characterized by low precipitations, by contrast, the most recent drought episodes were heat-driven drought (as mainly characterized by high temperatures) (Figs. 2; 3) (Park Williams et al., 2013). Although, previous studies have shown that “compound events”, characterized by low precipitation and high VPD, can trigger local and intense tree mortality episodes (Gazol and Camarero, 2022), in our study, it was likely that *Q. ilex* crown mortality was mainly imposed by the increment in temperatures regimes resulting in higher VPD values (Fig. 4; Fig. S1). Indeed, increment in VPD can be particularly stressful for plants, especially during the growing season, as VPD is the main driver for forest and soil evaporation (Grossiord et al., 2020; McDowell et al., 2020; Schwärzel et al., 2020). Accordingly, in the considered stands, differences in tree vigour among trees appeared only after 2017, when a loss of synchrony in growth rate between trees at D and ND sites was observed (Figs. 1; 5).

Quercus ilex at the Maremma Regional Park did not show a strong sensitivity to climate, as only few significant correlations were reported for trees at ND site and meteorological parameters (Table S8A).

In semi-arid ecosystems, water is the main limiting factor for plant growth (Cherubini et al., 2003; Martínez-vilalta et al., 2008; Pasho et al., 2012), and we expected that spring precipitation would have promoted an increase in RWI in the period 1988–2004 (Campelo et al., 2007, 2021; Granda et al., 2013; Camarero et al., 2021). Conversely, the increase in autumn and winter precipitation in the study area may have enhanced the positive effect of warm spring temperatures on tree growth (Campelo et al., 2009; Gea-Izquierdo et al., 2011; Abrantes et al., 2013) (Fig. 2; Table S2). Therefore, we suppose that precipitation plays a major role in *Q. ilex* radial growth after a period of limited water availability (Zalloni et al., 2018). Changes in the climate-growth relationship over time have been reported for several species (Carrer and Urbinati, 2006; Andreu et al., 2007; Gea-Izquierdo et al., 2009), including *Q. ilex*, whose growth response increment is linked to rising mean temperatures once it exceeds a threshold of approximately 600 mm of precipitation (Gea-

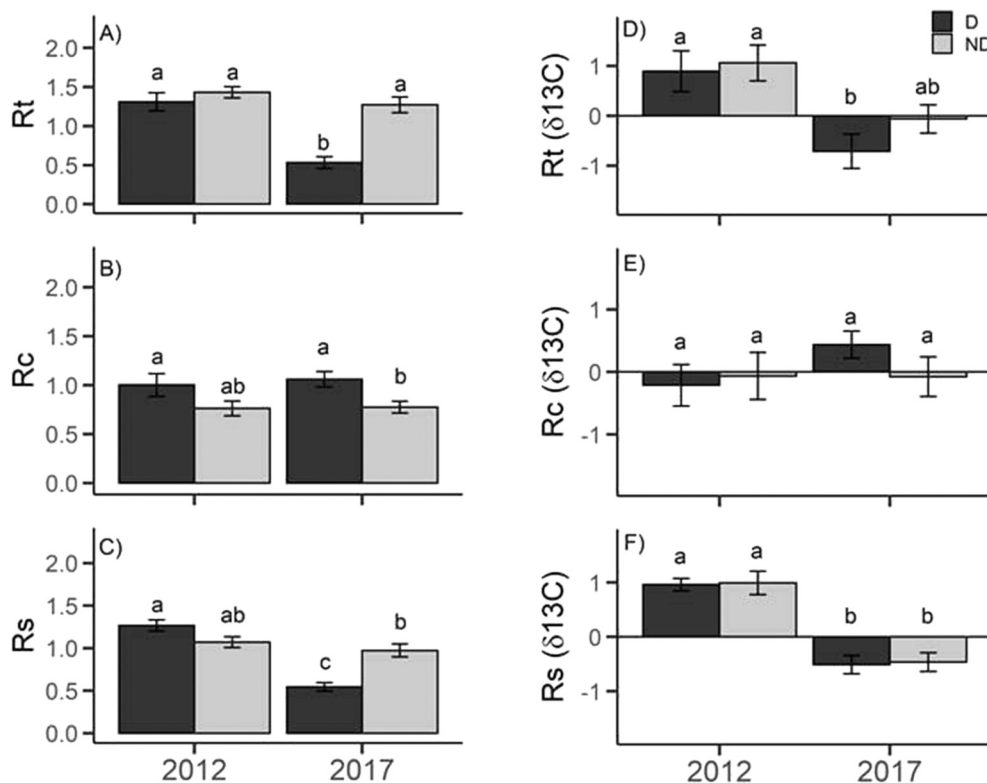


Fig. 7. Drought response indices: resistance, Rt and Rt ($\delta^{13}\text{C}$) (A, D); recovery, Rc and Rc ($\delta^{13}\text{C}$) (B, E); and resilience, Rs and Rs ($\delta^{13}\text{C}$) (C, F) of *Q. ilex* at declining (D) and non-declining (ND) sites. Indices were calculated for 2012 and 2017, considering \pm three years of the target years. Two-way ANOVA followed by Tukey's pairwise comparison was performed to compare data (mean \pm SE, $n = 5$ for Rt, Rc and Rs; $n = 4$ for Rt ($\delta^{13}\text{C}$), Rc ($\delta^{13}\text{C}$) and Rs ($\delta^{13}\text{C}$)). Letters represent significant differences between the responses of D and ND to drought events ($p < 0.05$).

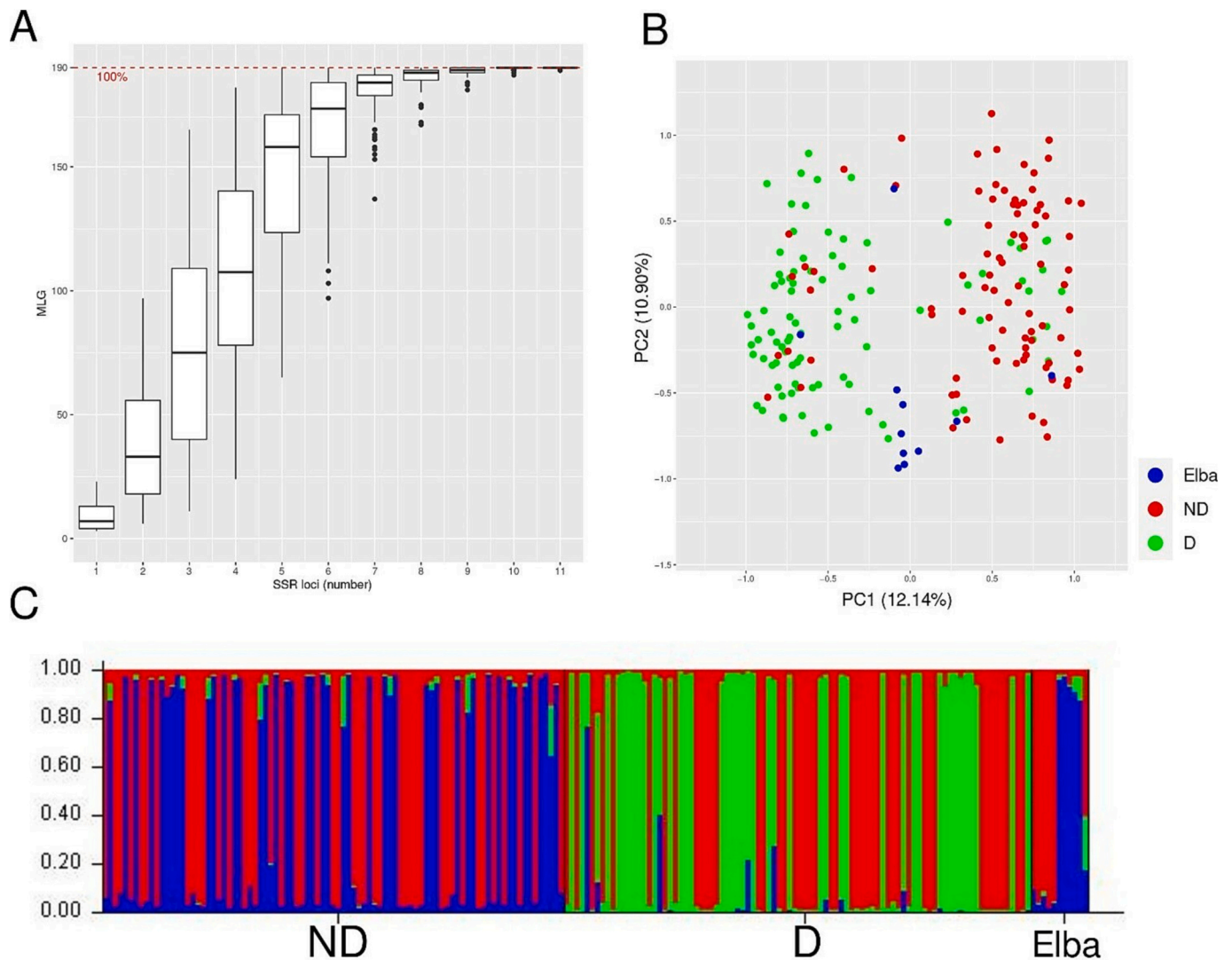


Fig. 8. SSR Genotyping Results. (A) Genotype accumulation curve showing the correlation between detected multi-locus genotypes (MLG) and the number of used SSR loci. (B) PCoA based on pairwise genetic distance matrix for all samples. (C) STRUCTURE analysis based on the genotyping outcomes: plot showing the probability that individuals (genotype) belong to one of the three inferred populations, including a population with individuals present in the three sites (red), a population harbouring individuals from ND and Elba (blue), and a population almost exclusively present in the D site (green). Each genotype is represented by a vertical line, which is partitioned into three coloured segments that represent the estimated membership of a distinct population.

Izquierdo et al., 2011). In contrast to *Q. ilex* trees at the ND site, radial growth at the D site appeared to be unresponsive to climatic variation. A similar behaviour was previously reported for *Pinus sylvestris* L. growing at an extremely dry site (Castellaneta et al., 2022). The authors have associated the reduced climatic responsiveness of the species to a long-term deterioration of hydraulic performance imposed by an unsafe water strategy and raising VPD in the study area. However, the relative influence of specific climate parameters on forest dieback is still poorly understood and several additional non-climatic factors may have potentially interfered with the climate signal recorded in tree-rings (i.e. massive defoliation through periodical outbreaks of herbivorous insects, oak masting) (Di Filippo et al., 2007; Büntgen et al., 2009; Black et al., 2016; Peltier and Ogle, 2020; Hacket-Pain and Bogdziewicz, 2021; Fuchs et al., 2021). The influence of such sporadic factors on radial growth was not tested in our study. Furthermore, the deep root-system of Mediterranean oaks, enabling them to access to deep ground water reserves, may have contributed to the weak responsiveness of radial growth to precipitation regime (Zadworny et al., 2019; Carrière et al., 2020; Ripullone et al., 2020). In addition, previous studies have shown that higher temperatures in the last decades led to non-linear patterns of

tree growth responses to climatic variations in Mediterranean species (Lebourgeois et al., 2012).

Tree-ring $\delta^{13}\text{C}$ can be used to investigate variations in plant WUE_i between different species and genotypes, and their responses to climatic pressures (Shestakova and Martínez-Sancho, 2021). We observed a declining $\delta^{13}\text{C}$ trend at both sites, which could be partly related to the precipitation pattern, indicating a reduction in drought stress conditions (Fig. 6; Table S2). Indeed, when higher precipitation occurs, as in our study area after 2004, trees' ability to discriminate against ^{13}C is improved (Francey and Farquhar, 1982; McCarroll & Loader, 2004). Furthermore, previous studies have shown that the low values of tree-ring $\delta^{13}\text{C}$ in the current year may be associated with the mobilization of starch reserves (Jäggi et al., 2002; Helle and Schleser, 2004a; Shestakova et al., 2014). Thus, we did not exclude that the low inter-annual variability of the $\delta^{13}\text{C}$ signal may be due to tree consumption of carbohydrate reserves, instead of the utilization of fresh assimilated carbon or a mixing of stored and fresh carbon pools (Keel et al., 2007). However, $\delta^{13}\text{C}$ at ND significantly exceeded that observed at site D over almost the entire study period, revealing a more conservative use of water for *Q. ilex* at the ND site than D site (Puchi et al., 2021). Thus, the

less conservative use of water for *Q. ilex* at D site supports the hypothesized long-term deterioration of hydraulic performance, as previously mentioned (Castellaneta et al., 2022). In addition, the negative correlation observed between $\delta^{13}\text{C}$ -chronology, and annual and winter T_{\min} at the ND site may suggest an alleviation of low-temperature limitations (Table S2, Table S10). In detail, warmer temperatures in the cold season may have induce an increase in photosynthetic rates and stomatal conductance in Mediterranean evergreens during winter, when the low values of VPD and the grate variability of precipitations guarantee to *Q. ilex* a safe use of water (Prieto et al., 2009; Klein et al., 2013). On the other hand, $\delta^{13}\text{C}$ is also affected by changes in photosynthetic activity, which may be affected by nutritional or irradiance stress (Yakir and Israeli, 1995; Livingston et al., 1998). Thus, higher $\delta^{13}\text{C}$ values could be linked to a safer use of water, higher photosynthetic capacity, or both in combination (Scheidegger et al., 2000; Ferrio et al., 2003). This second interpretation would attribute a higher photosynthetic capacity to *Q. ilex* at the ND site, which may potentially explain the negative correlation between annual and summer T_{mean} , T_{max} , and autumn T_{max} with $\delta^{13}\text{C}$ -chronology (Table S10) (Montserrat-Martí et al., 2009). This is also consistent with the higher growth rates observed at the ND site in some years. After all, *Q. ilex* at the ND site exhibited dependence on the isotopic signal in the temperature regime rather than in the precipitation regime, as previously observed by Shestakova et al. (2014). Overall, *Q. ilex* tree-ring $\delta^{13}\text{C}$ at the Maremma Regional Park showed a weak climate signal, as already observed for RWI. A further potential factor that may have reduced tree-ring $\delta^{13}\text{C}$ sensitivity environmental signals concern *Q. ilex* multi-stemmed growth form (Table S4). Thus, both intra- and inter-plant competitions may have weakened $\delta^{13}\text{C}$ climatic signals in our study (Farahat et al., 2022; Pasquini et al., 2023). However, the two stands showed similar $\delta^{13}\text{C}$ only in 2018 when $\delta^{13}\text{C}$ increased only at the D site, thus suggesting that the drought in 2017 may have had a stronger impact on D trees compared to ND trees.

4.2. Resistance, recovery and resilience of *Q. ilex* to drought

The intense drought in 2017 significantly impaired *Q. ilex* growth at the D site, which was less resistant (Rt) and resilient (Rs) to drought stress compared to trees at the ND site. Loss of resilience after severe dry spells (i.e., in 2017) is associated with an increased risk of tree mortality (DeSoto et al., 2020). Further, the hypothesis of the presence of a trade-off between tree-ring-growth resistance and recovery after drought was partially confirmed in our study, as the highest growth recovery (Rc) was recorded concomitantly with the lowest Rs value only in 2017 at the D site (Galiano et al., 2011; Leite et al., 2019) (Fig. 7 A, C). A recent meta-analysis reported that trees that died due to water shortages are not as capable of recovering from previous non-lethal droughts as other trees of the same species (DeSoto et al., 2020). These findings support the hypothesis that the ability of trees to recover from drought is an important factor that determines their overall resilience (DeSoto et al., 2020). However, D and ND trees did not differ for the radial growth resistance, recovery and resilience considering the mild drought in 2012 (Fig. 7 A, B, C). Therefore, we may consider 2017 as the starting year for *Q. ilex* dieback in our study area. Indeed, 2017 was a peculiar year for the meteorology of Tuscany and of the entire Italian peninsula, in which episodes of forest dieback and intense defoliation strongly increased at a regional and national level (Pollastrini et al., 2019; Puletti et al., 2019; Bussotti et al., 2022). Similar to the drought response indices based on radial growth, no differences emerged between the D and ND sites considering the indices calculated using $\delta^{13}\text{C}$ data in 2012 (Fig. 7 D, E, F). Nonetheless, the intense drought in 2017 significantly affected *Q. ilex* physiology in the study area because negative values of resistance indices calculated from $\delta^{13}\text{C}$ data (Rt ($\delta^{13}\text{C}$)) suggest lower discrimination against ^{13}C (Shestakova et al., 2014). Although we did not apply a dual isotope approach, it is unlikely that such an increase in tree-ring ^{13}C in 2017 could be associated with an increase in photosynthetic capacity, as reductions in the maximum carboxylation rate and stomatal and

mesophyll conductance are often observed in *Q. ilex* subjected to drought stress (Limousin et al., 2010; Alonso-Forn et al., 2021). Nonetheless, only trees at the D site showed a significant decrease in Rt($\delta^{13}\text{C}$) from 2012 to 2017, highlighting the greater impact of drought on trees located at the D site (Fig. 7 D). The alteration in stomatal regulation imposed by drought in 2017 lasted for at least three years at both sites, as suggested by the significant reduction in Rs($\delta^{13}\text{C}$) from 2012 to 2017 at both sites (Fig. 7 F). Therefore, intense drought can alter tree physiology for several years or cause permanent changes in tree performance (Galiano et al., 2012; Gessler et al., 2020). Despite the similar impact of drought 2017 on Rs($\delta^{13}\text{C}$) at the D and ND sites, significant differences emerged in $\delta^{13}\text{C}$ -chronologies of trees at both sites could partially be explained by the analysis of the population structure.

4.3. Genotyping provides evidence that dieback is genetically determined

The population structure analysis based on genotyping outcomes suggested the presence of three *Q. ilex* sub-populations within the analysed samples: a first detected at Elba Island, D and ND sites; a second at ND site and in Elba Island; and the last found exclusively at D site (Fig. 8). Diversity indices demonstrated that the three populations had high genetic diversity, as high values of unbiased allelic diversity *per* locus were detected. The main factor that may have contributed to the increase in allele and genotype diversity was probably gene flow among the D, ND, and Elba sites. These outcomes might be the result of pollen movement that over time caused gene flow between trees on Maremma and those on Elba Island. Studies on pollen from *Quercus* spp. have shown that it may travel by wind across significant distances, for example >100 km, reaching the upper layers of the atmosphere (Kremer et al., 2010). In addition, cumulative rotational grazing has been used in Italian forests, particularly in the oak forests of Maremma, to provide charcoal and timber for pasture (Manetti et al., 2009). Past forest management practices, environmental and climatic disturbances may promote *Q. ilex* resprouting over sexual reproduction, thus contributing to the maintenance of genetic variability between the two stands (Valbuena-Carabaña et al., 2008; Ortego et al., 2010). Since Maremma Regional Park was designated a protected area in 1975, less anthropic activity has impacted the area in the last 50 years, enabling plants to grow and reproduce freely and promoting an increase in genetic variability throughout the range. However, we cannot rule out the possibility that the population structure of *Q. ilex* at the sites could be the result of *Q. ilex* hybridization with other *Quercus* species, as previously reported (Burgarella et al., 2009; Backs et al., 2016). This aspect, beyond the purpose of the current study, which aimed to assess the presence of a link between genotypes and phenotypes with drought-induced crown damage, will be further explored using dedicated molecular approaches (Maldonado-Alconada et al., 2022).

By analyzing the results from the SSR genotyping and $\delta^{13}\text{C}$ analysis, it is worth noting that all the samples collected at D and ND used for $\delta^{13}\text{C}$ analysis were assigned to two distinct sub-populations (one detected only at D and the other found at D, ND, and Elba Island) (Tables S12, S13), supporting the hypothesis that the observed differences in $\delta^{13}\text{C}$ -chronologies may have a genetic basis (Rousset et al., 2009).

The successful genotyping of all analysed trees was achieved thanks to the use of a novel set of 11 nuclear and chloroplast SSR markers, coupled with HRM analysis. The application of HRM was an efficient alternative of electrophoresis-based method for SSR scoring, as previously reported in other population genetic studies on trees (Distefano et al., 2012). Because a limited number of SSR may affect the resolution of genotyping in *Q. ilex*, it is crucial to analyse a large number of molecular markers to optimize the genotyping step (Savi et al., 2019). Genetic studies using a large number of molecular markers, including Single Nucleotide Polymorphisms (SNPs; Fasanella et al., 2021) and Inter Simple Sequence Repeats (ISSRs; Shamari et al., 2018), have previously proven to be effective in detecting a link between phenotypic and genetic variations related with drought response in different tree

species. The importance of using an appropriate number of genetic molecular markers in genotyping studies of forest species was further underlined by our findings, which demonstrated that the use of SSR markers can reveal changes in population structure between D and ND trees (Venegas-González et al., 2022). In our case, genetic differences fit with $\delta^{13}\text{C}$ -chronologies, which revealed the presence of high and low WUE_i phenotypes at ND and D sites, respectively. Notably, different genotypes of sessile oak have been associated with different phenotypes, with high and low WUE_i values (Le Provost et al., 2022).

Although the divergence between $\delta^{13}\text{C}$ -chronologies may be partially explained by different water/nutrient availability understory composition between the two sites (Table S1) (Pasquini et al., 2023), our results strongly support the hypothesis that different *Q. ilex* subpopulations may have had different physiological responses to environmental stresses. The genetic control of the isotopic signature was also highlighted by Roussel et al. (2009), who found important differences in stomatal density and diurnal courses of stomatal conductance comparing *Quercus robur* L. genotypes with “high” and “low” $\delta^{13}\text{C}$ in bulk leaf matter, wood, and cellulose in wood. The combination of tree-ring $\delta^{13}\text{C}$ with genetic data has already proven to be a promising approach to investigate the prospects of artificial stands for ex situ conservation (Santini et al., 2020); therefore, we suggest its use in the selection of drought-tolerant genotypes of seed-bearing plants to preserve Mediterranean holm oak ecosystem types. It should be noted that the association of drought with pathogenic infections may have a destructive impact on Mediterranean oak forest ecosystems (Corcobado et al., 2014). In particular, the interaction of pathogens such as *P. cinammonni* or *Biscogniauxia* spp. with drought events can make *Q. ilex* particularly susceptible to dieback, even in the case of non-lethal infections (Corcobado et al., 2013; Ruiz-Gómez et al., 2019; San-Eufrasio et al., 2021; Encinas-Valero et al., 2022). In this context, further studies are needed to assess whether SSR genotyping can also be applied to select trees putatively tolerant to biotic stressors.

5. Conclusion

In conclusion, the growth rate of *Q. ilex* at D site was lower than that at ND site, but significant differences were observed only in few years, thus only partially confirming the first hypothesis. Our results strongly support the hypothesized difference in tree-ring $\delta^{13}\text{C}$ signals between the D and ND trees. Indeed, the substantial divergence in $\delta^{13}\text{C}$ signals between the two stands suggests a water-saving behaviour for *Q. ilex* at the ND site as opposed to a less conservative use of water for *Q. ilex* at the D site, which helps ND trees survive under these harsh conditions. Despite the proximity of the stands, significant correlations with climatic parameters, ring-width patterns, and $\delta^{13}\text{C}$ chronology were found only at the ND site. Therefore, we conclude that trees at D site are less responsive to seasonal climatic variations than trees at the ND site. Nonetheless, the divergence in $\delta^{13}\text{C}$ signals between trees at the D and ND sites is in accordance with the presumed different susceptibility of the two stands to drought-induced mortality based on genetic bias, thus confirming our third hypothesis. *Q. ilex* at ND resulted more resistant and resilient to drought than trees at the D site, probably because of its conservative water use. To the best of our knowledge, this is the first study showing intraspecific differences in the genotypic and phenotypic levels of drought response in *Q. ilex* trees grown in the same environment. Future research could examine whether the genetic differences observed between *Q. ilex* at the D and ND sites would correspond to physiological differences in the offspring. Furthermore, it would be interesting to deepen the study of the relationship between specific microenvironmental factors of the D and ND sites and the spatial genetic structure of *Q. ilex* in the study area. This study underlines the potential of combining $\delta^{13}\text{C}$ analysis with SSR genotyping as a powerful tool for identifying trees putatively tolerant to water deficit. Such a method may also be used in the selection of genotypes for seed-bearing plants to preserve Mediterranean holm oak ecosystem types.

CRedit authorship contribution statement

Conceptualization: C. Brunetti, P. Cherubini, R. Balestrini. **Investigation:** F. Alderotti, C. Brunetti, A. Gori, D. Pasquini. **Methodology:** F. Alderotti, F. Sillo, R. Inghes, M. Saurer, L. Brilli. **Data curation:** F. Alderotti, F. Sillo, M. Saurer, L. Brilli. **Formal analysis:** F. Alderotti, F. Sillo, L. Brilli, F. Bussotti, M. Centritto, F. Ferrini, A. Gori, R. Inghes, D. Pasquini, M. Pollastrini, M. Saurer, P. Cherubini, R. Balestrini, C. Brunetti. **Writing** – original draft: F. Alderotti, F. Sillo, C. Brunetti, R. Balestrini, P. Cherubini; **Writing** – review & editing: all the authors. **Supervision:** C. Brunetti, R. Balestrini, P. Cherubini; **Resource acquisition:** M. Centritto, F. Ferrini, F. Bussotti.

Declaration of competing interest

The authors declare that they have no known competing financial interests or personal relationships that could have appeared to influence the work reported in this paper.

Data availability

Data will be made available on request.

Acknowledgements

The authors are grateful to Maremma Regional Park to have allowed access to the study area in the frame of the project "Impatto dei cambiamenti climatici sulla vegetazione di ecosistemi costieri mediterranei", and thank Dr. Lorenzo Chelazzi and Dr. Laura Tonelli for their help in the collection of plant samples. This study was supported by the Society for Experimental Biology (SEB) with the Company of Biologists travel grant, a grant supporting early career scientist SEB members with taking part in research trips. The author acknowledges the support of NBFC to University of Firenze, Department of Agriculture, Food, Environment and Forestry, funded by the Italian Ministry of University and Research, PNRR, Missione 4 Componente 2, “Dalla ricerca all’impresa”, Investimento 1.4, Project CN000000033

Appendix A. Supplementary data

Supplementary data to this article can be found online at <https://doi.org/10.1016/j.scitotenv.2023.166809>.

References

- Abrantes, J., Campelo, F., García-González, I., Nabais, C., 2013. Environmental control of vessel traits in *Quercus ilex* under Mediterranean climate: relating xylem anatomy to function. *Trees* 27, 655–662. <https://doi.org/10.1007/s00468-012-0820-6>.
- Adams, H.D., Zeppel, M.J., Anderegg, W.R., Hartmann, H., Landhäusser, S.M., Tissue, D. T., Anderegg, L.D., 2017. A multi-species synthesis of physiological mechanisms in drought-induced tree mortality. *Nat. Ecol. Evol.* 1 (9), 1285–1291. <https://doi.org/10.1038/s41559-017-0248-x>.
- Alderotti, F., Verdiani, E., 2023. God save the queen! How and why the dominant evergreen species of the Mediterranean Basin is declining? *AoB Plants* plad051. <https://doi.org/10.1093/aobpla/plad051>.
- Alonso-Forn, D., Peguero-Pina, J.J., Ferrio, J.P., Mencuccini, M., Mendoza-Herrer, Ó., Sancho-Knapik, D., Gil-Pelegrín, E., 2021. Contrasting functional strategies following severe drought in two Mediterranean oaks with different leaf habit: *Quercus faginea* and *Quercus ilex* subsp. *rotundifolia*. *Tree Physiol.* 41 (3), 371–387. <https://doi.org/10.1093/treephys/tpaa135>.
- Anderegg, W.R., Schwalb, C., Biondi, F., Camarero, J.J., Koch, G., Litvak, M., Pacala, S., 2015. Pervasive drought legacies in forest ecosystems and their implications for carbon cycle models. *Science* 349 (6247), 528–532. <https://doi.org/10.1007/s00704-022-04019-2>.
- Andreu, L., Gutierrez, E., Macias, M., Ribas, M., Bosch, O., Camarero, J.J., 2007. Climate increases regional tree-growth variability in Iberian pine forests. *Glob. Chang. Biol.* 13 (4), 804–815. <https://doi.org/10.1111/j.1365-2486.2007.01322.x>.
- Backs, J.R., Terry, M., Ashley, M.V., 2016. Using genetic analysis to evaluate hybridization as a conservation concern for the threatened species *Quercus hinckleyi* C. H. muller. (Fagaceae). *International Journal of. Plant Sci.* 177 (2), 122–131. <https://doi.org/10.1086/684177>.

- Barbata, A., Ogaya, R., Peñuelas, J., 2013. Dampening effects of long-term experimental drought on growth and mortality rates of a Holm oak forest. *Glob. Chang. Biol.* 19 (10), 3133–3144. <https://doi.org/10.1111/gcb.12269>.
- Bartholomé, J., Mabilia, A., Savelli, B., Bert, D., Brendel, O., Plomion, C., Gion, J.M., 2015. Genetic architecture of carbon isotope composition and growth in *Eucalyptus* across multiple environments. *New Phytol.* 206 (4), 1437–1449. <https://doi.org/10.1111/nph.13301>.
- Battipaglia, G., De Micco, V., Brand, W.A., Saurer, M., Aronne, G., Linke, P., Cherubini, P., 2014. Drought impact on water use efficiency and intra-annual density fluctuations in *Erica arborea* on Elba (Italy). *Plant Cell Environ.* 37 (2), 382–391. <https://doi.org/10.1111/pce.12160>.
- Black, B.A., Griffin, D., van der Sleen, P., Wanamaker Jr., A.D., Speer, J.H., Frank, D.C., Gillanders, B.M., 2016. The value of crossdating to retain high-frequency variability, climate signals, and extreme events in environmental proxies. *Glob. Chang. Biol.* 22 (7), 2582–2595. <https://doi.org/10.1111/gcb.13256>.
- Brendel, O., Epron, D., 2022. Are differences among forest tree populations in carbon isotope composition an indication of adaptation to drought? *Tree Physiol.* 42 (1), 26–31. <https://doi.org/10.1093/treephys/tpab143>.
- Bunn, A., Korpela, M., Biondi, F., Campelo, F., Mérian, P., Qeadan, F., Schulz, M., 2021. Package ‘dplR’. Retrieved from. <https://cran.r-project.org/web/packages/dplR/dpIR.pdf>.
- Büntgen, U., Frank, D., Liebhold, A., Johnson, D., Carrer, M., Urbanini, C., Esper, J., 2009. Three centuries of insect outbreaks across the European alps. *New Phytol.* 182 (4), 929–941. <https://doi.org/10.1111/j.1469-8137.2009.02825.x>.
- Buras, A., 2017. A comment on the expressed population signal. *Dendrochronologia* 44, 130–132. <https://doi.org/10.1016/j.dendro.2017.03.005>.
- Burgarella, C., Lorenzo, Z., Jabbour-Zahab, R., Lumaret, R., Guichoux, E., Petit, R.J., Gil, L., 2009. Detection of hybrids in nature: application to oaks (*Quercus suber* and *Q. ilex*). *Heredity* 102 (5), 442–452. <https://doi.org/10.1038/hdy.2009.8>.
- Bussotti, F., Papitto, G., Di Martino, D., Cocciuffa, C., Cindolo, C., Cenni, E., Bettini, D., Iacopetti, G., Pollastrini, M., 2022. Le condizioni delle foreste italiane stanno peggiorando a causa di eventi climatici estremi? Evidenze dalle reti di monitoraggio nazionali ICP Forests-CON. *ECO. FOR. Forest* 19 (1), 74. <https://doi.org/10.3832/efor4134-019>.
- Camarero, J.J., Gazol, A., Sangüesa-Barreda, G., Oliva, J., Vicente-Serrano, S.M., 2015. To die or not to die: early warnings of tree dieback in response to a severe drought. *J. Ecol.* 103 (1), 44–57. <https://doi.org/10.1111/1365-2745.12295>.
- Camarero, J.J., Sangüesa-Barreda, G., Vergarechea, M., 2016. Prior height, growth, and wood anatomy differently predispose to drought-induced dieback in two Mediterranean oak species. *Ann. For. Sci.* 73 (2), 341–351. <https://doi.org/10.1007/s13595-015-0523-4>.
- Camarero, J.J., Rubio-Cuadrado, Á., Gazol, A., 2021. Climate windows of intra-annual growth and post-drought recovery in Mediterranean trees. *Agric. For. Meteorol.* 308, 108606. <https://doi.org/10.1016/j.agrformet.2021.108606>.
- Campelo, F., Gutiérrez, E., Ribas, M., Nabais, C., Freitas, H., 2007. Relationships between climate and double rings in *Quercus ilex* from northeast Spain. *Can. J. For. Res.* 37 (10), 1915–1923. <https://doi.org/10.1139/X07-050>.
- Campelo, F., Nabais, C., García-González, I., Cherubini, P., Gutiérrez, E., Freitas, H., 2009. Dendrochronology of *Quercus ilex* L. and its potential use for climate reconstruction in the Mediterranean region. *Can. J. For. Res.* 39 (12), 2486–2493. <https://doi.org/10.1139/X09-163>.
- Campelo, F., Nabais, C., Gutiérrez, E., Freitas, H., García-González, I., 2010. Vessel features of *Quercus ilex* L. growing under Mediterranean climate have a better climatic signal than tree-ring width. *Trees* 24, 463–470. <https://doi.org/10.1007/s00468-010-0414-0>.
- Campelo, F., Ribas, M., Gutiérrez, E., 2021. Plastic bimodal growth in a Mediterranean mixed-forest of *Quercus ilex* and *Pinus halepensis*. *Dendrochronologia* 67, 125836. <https://doi.org/10.1016/j.dendro.2021.125836>.
- Carrer, M., Urbanini, C., 2006. Long-term change in the sensitivity of tree-ring growth to climate forcing in *Larix decidua*. *New Phytol.* 170 (4), 861–872. <https://doi.org/10.1111/j.1469-8137.2006.01703.x>.
- Carrière, S.D., Martin-StPaul, N.K., Cakpo, C.B., Patris, N., Gillon, M., Chalikakis, K., Davi, H., 2020. The role of deep vadose zone water in tree transpiration during drought periods in karst settings—insights from isotopic tracing and leaf water potential. *Sci. Total Environ.* 699, 134332. <https://doi.org/10.1016/j.scitotenv.2019.134332>.
- Castellana, M., Rita, A., Camarero, J.J., Colangelo, M., Ripullone, F., 2022. Declines in canopy greenness and tree growth are caused by combined climate extremes during drought-induced dieback. *Sci. Total Environ.* 813, 152666. <https://doi.org/10.1016/j.scitotenv.2021.152666>.
- Cherubini, P., Gartner, B.L., Tognetti, R., Braeker, O.U., Schoch, W., Innes, J.L., 2003. Identification, measurement, and interpretation of tree rings in woody species from Mediterranean climates. *Biol. Rev.* 78 (1), 119–148. <https://doi.org/10.1017/S1464793102006000>.
- Cherubini, P., Battipaglia, G., Innes, J.L., 2021. Tree vitality and forest health: can tree-ring stable isotopes be used as indicators? *Curr. For. Rep.* 7, 69–80. <https://doi.org/10.1007/s40725-021-00137-8>.
- Colangelo, M., Camarero, J.J., Ripullone, F., Gazol, A., Sánchez-Salguero, R., Oliva, J., Redondo, M.A., 2018. Drought decreases growth and increases mortality of coexisting native and introduced tree species in a temperate floodplain forest. *Forests* 9 (4), 205. <https://doi.org/10.3390/f9040205>.
- Corcobado, T., Cubera, E., Moreno, G., Solla, A., 2013. *Quercus ilex* forests are influenced by annual variations in water table, soil water deficit and fine root loss caused by *Phytophthora cinnamomi*. *Agric. For. Meteorol.* 169, 92–99. <https://doi.org/10.1016/j.agrformet.2012.09.017>.
- Corcobado, T., Cubera, E., Juárez, E., Moreno, G., Solla, A., 2014. Drought events determine performance of *Quercus ilex* seedlings and increase their susceptibility to *Phytophthora cinnamomi*. *Agric. For. Meteorol.* 192, 1–8. <https://doi.org/10.1016/j.agrformet.2014.02.007>.
- Corcuera, L., Camarero, J.J., Gil-Pelegrín, E., 2004. Effects of a severe drought on *Quercus ilex* radial growth and xylem anatomy. *Trees* 18 (1), 83–92. <https://doi.org/10.1007/s00468-003-0284-9>.
- David, T.S., Henriques, M.O., Kurz-Besson, C., Nunes, J., Valente, F., Vaz, M., David, J.S., 2007. Water-use strategies in two co-occurring Mediterranean evergreen oaks: surviving the summer drought. *Tree Physiol.* 27 (6), 793–803. <https://doi.org/10.1093/treephys/27.6.793>.
- Deguilloux, M.F., Pemonge, M.H., Petit, R.J., 2004. Use of chloroplast microsatellites to differentiate oak populations. *Ann. For. Sci.* 61 (8), 825–830. <https://doi.org/10.1051/forest:2004078>.
- DeSoto, L., Cailleret, M., Sterck, F., Jansen, S., Kramer, K., Robert, E.M.R., Aakala, T., Amoroso, M.M., Bigler, C., Camarero, J.J., Cufar, K., Gea-Izquierdo, G., Gillner, S., Haavik, L.J., Hereş, A.-M., Kane, J.M., Kharuk, V.I., Kitzberger, T., Klein, T., Martínez-Vilalta, J., 2020. Low growth resilience to drought is related to future mortality risk in trees. *Nat. Commun.* 11, 1–9. <https://doi.org/10.1038/s41467-020-14300>.
- Di Filippo, A., Biondi, F., Cufar, K., De Luis, M., Grabner, M., Maugeri, M., Piovesan, G., 2007. Bioclimatology of beech (*Fagus sylvatica* L.) in the Eastern Alps: spatial and altitudinal climatic signals identified through a tree-ring network. *J. Biogeogr.* 34 (11), 1873–1892. <https://doi.org/10.1111/j.1365-2699.2007.01747.x>.
- Distefano, G., Caruso, M., La Malfa, S., Gentile, A., Wu, S.B., 2012. High resolution melting analysis is a more sensitive and effective alternative to gel-based platforms in analysis of SSR—an example in citrus. *PLoS One* 7 (8), e44202. <https://doi.org/10.1371/journal.pone.0044202>.
- Du, L., Li, Y., Zhang, X., Yue, B., 2013. MSDB: a user-friendly program for reporting distribution and building databases of microsatellites from genome sequences. *J. Hered.* 104 (1), 154–157. <https://doi.org/10.1093/jhered/ess082>.
- Earl, D.A., VonHoldt, B.M., 2012. STRUCTURE HARVESTER: a website and program for visualizing STRUCTURE output and implementing the Evanno method. *Conserv. Genet. Resour.* 4 (2), 359–361. <https://doi.org/10.1007/s12686-011-9548-7>.
- Encinas-Valero, M., Esteban, R., Hereş, A.M., Vivas, M., Fakhret, D., Aranjuelo, I., Curiel Yuste, J., 2022. Holm oak decline is determined by shifts in fine root phenotypic plasticity in response to belowground stress. *New Phytol.* 235 (6), 2237–2251. <https://doi.org/10.1111/nph.18182>.
- Farahat, E., Cherubini, P., Saurer, M., Gärtner, H., 2022. Wood anatomy and tree-ring stable isotopes indicate a recent decline in water-use efficiency in the desert tree *Moringa peregrina*. *Int. J. Biometeorol.* 1–11. <https://doi.org/10.1007/s00484-021-02198-7>.
- Farquhar, G.D., Ehleringer, J.R., Hubick, K.T., 1989. Carbon isotope discrimination and photosynthesis. *Annu. Rev. Plant Biol.* 40 (1), 503–537.
- Farquhar, M.H., O'Leary, J.A., Berry, 1982. On the relationship between carbon isotope discrimination and intercellular carbon dioxide concentration in leaves. *Aust. J. Plant Physiol.* 9, 121–137.
- Fasanella, M., Suarez, M.L., Hasbun, R., Premoli, A.C., 2021. Individual-based dendrochronological analysis of forest dieback driven by extreme droughts. *Can. J. For. Res.* 51 (3), 420–432. <https://doi.org/10.1139/cjfr-2020-0221>.
- Fernández i Martí, A., Romero-Rodríguez, C., Navarro-Cerrillo, R.M., Abril, N., Jorrín-Novo, J.V., Dodd, R.S., 2018. Population genetic diversity of *Quercus ilex* subsp. *ballota* (Desf.) Samp. reveals divergence in recent and evolutionary migration rates in the Spanish dehesas. *Forests* 9 (6), 337. <https://doi.org/10.3390/f9060337>.
- Ferrio, J.P., Florit, A., Vega, A., Serrano, L., Voltas, J., 2003. $\delta^{13}C$ and tree-ring width reflect different drought responses in *Quercus ilex* and *Pinus halepensis*. *Oecologia* 137 (4), 512–518. <https://doi.org/10.1007/s00442-003-1372-7>.
- Ferrio, J.P., Shestakova, T.A., del Castillo, J., Voltas, J., 2021. Oak competition dominates interspecific interactions in growth and water-use efficiency in a mixed pine-oak Mediterranean forest. *Forests* 12 (8), 1093. <https://doi.org/10.3390/f12081093>.
- Fluch, S., Turetschek, E., Lexer, C., Streiff, R., Kremer, A., Burg, K., Glössl, J., 1997. Identification and characterization of (GA/CT) n-microsatellite loci from *Quercus petraea*. *Plant Mol. Biol.* 33 (6), 1093–1096. <https://doi.org/10.1023/A:1005736722294>.
- Fonti, P., von Arx, G., García-González, I., Eilmann, B., Sass-Klaassen, U., Gärtner, H., Eckstein, D., 2010. Studying global change through investigation of the plastic responses of xylem anatomy in tree rings. *New Phytol.* 185 (1), 42–53. <https://doi.org/10.1111/j.1469-8137.2009.03030.x>.
- Francey, R.J., Farquhar, G.D., 1982. An explanation of $^{13}C/^{12}C$ variations in tree rings. *Nature* 297 (5861), 28–31. <https://doi.org/10.1038/297028a0>.
- Fuchs, S., Schuldt, B., Leuschner, C., 2021. Identification of drought-tolerant tree species through climate sensitivity analysis of radial growth in central European mixed broadleaf forests. *For. Ecol. Manag.* 494, 119287. <https://doi.org/10.1016/j.foreco.2021.119287>.
- Galiano, L., Martínez-Vilalta, J., Lloret, F., 2011. Carbon reserves and canopy defoliation determine the recovery of Scots pine 4 yr after a drought episode. *New Phytol.* 190 (3), 750–759. <https://doi.org/10.1111/j.1469-8137.2010.03628.x>.
- Galiano, L., Martínez-Vilalta, J., Sabatés, S., Lloret, F., 2012. Determinants of drought effects on crown condition and their relationship with depletion of carbon reserves in a Mediterranean holm oak forest. *Tree Physiol.* 32 (4), 478–489. <https://doi.org/10.1093/treephys/tps025>.
- García-Angulo, D., Hereş, A.M., Fernández-López, M., Flores, O., Sanz, M.J., Rey, A., Yuste, J.C., 2020. Holm oak decline and mortality exacerbates drought effects on soil biogeochemical cycling and soil microbial communities across a climatic gradient. *Soil Biol. Biochem.* 149, 107921. <https://doi.org/10.1016/j.soilbio.2020.107921>.

- Gavinet, J., Ourcival, J.M., Gauzere, J., de Jalón, L.G., Limousin, J.M., 2020. Drought mitigation by thinning: benefits from the stem to the stand along 15 years of experimental rainfall exclusion in a holm oak coppice. *For. Ecol. Manag.* 473, 118266 <https://doi.org/10.1016/j.foreco.2020.118266>.
- Gazol, A., Camarero, J.J., 2022. Compound climate events increase tree drought mortality across European forests. *Sci. Total Environ.* 816, 151604 <https://doi.org/10.1016/j.scitotenv.2021.151604>.
- Gazol, A., Ribas, M., Gutiérrez, E., Camarero, J.J., 2017. Aleppo pine forests from across Spain show drought-induced growth decline and partial recovery. *Agric. For. Meteorol.* 232, 186–194. <https://doi.org/10.1016/j.agrformet.2016.08.014>.
- Gea-Izquierdo, G., Martín-Benito, D., Cherubini, P., Isabel, C., 2009. Climate-growth variability in *Quercus ilex* L. west Iberian open woodlands of different stand density. *Ann. For. Sci.* 66 (8), 802. <https://doi.org/10.1051/forest/2009080>.
- Gea-Izquierdo, G., Cherubini, P., Cañellas, I., 2011. Tree-rings reflect the impact of climate change on *Quercus ilex* L. along a temperature gradient in Spain over the last 100 years. *For. Ecol. Manag.* 262 (9), 1807–1816. <https://doi.org/10.1016/j.foreco.2011.07.025>.
- Gentilesca, T., Camarero, J.J., Colangelo, M., Nole, A., Ripullone, F., 2017. Drought-induced oak decline in the western Mediterranean region: an overview on current evidences, mechanisms and management options to improve forest resilience. *iForest-Biogeosci. For.* 10 (5), 796. <https://doi.org/10.3832/for2317-010>.
- Gessler, A., Bottero, A., Marshall, J., Arend, M., 2020. The way back: recovery of trees from drought and its implication for acclimation. *New Phytol.* 228 (6), 1704–1709. <https://doi.org/10.1111/nph.16703>.
- Giorgi, F., 2006. Climate change hot-spots. *Geophys. Res. Lett.* 33 (8) <https://doi.org/10.1029/2006GL025734>.
- Gomes, S., Breia, R., Carvalho, T., Carnide, V., Martins-Lopes, P., 2018. Microsatellite high-resolution melting (SSR-HRM) to track olive genotypes: from field to olive oil. *J. Food Sci.* 83 (10), 2415–2423. <https://doi.org/10.1111/1750-3841.14333>.
- González-Rodríguez, V., Navarro-Cerrillo, R.M., Villar, R., 2011. Artificial regeneration with *Quercus ilex* L. and *Quercus suber* L. by direct seeding and planting in southern Spain. *Ann. For. Sci.* 68, 637–646. <https://doi.org/10.1007/s13595-011-0057-3>.
- Goodstein, D.M., Shu, S., Howson, R., Neupane, R., Hayes, R.D., Fazo, J., Rokhsar, D.S., 2012. Phytome: a comparative platform for green plant genomics. *Nucleic Acids Res.* 40 (D1), D1178–D1186. <https://doi.org/10.1093/nar/gkr944>.
- Gori, A., Moura, B.B., Sillo, F., Alderotti, F., Pasquini, D., Balestrini, R., Brunetti, C., 2023. Unveiling resilience mechanisms of *Quercus ilex* seedlings to severe water stress: changes in non-structural carbohydrates, xylem hydraulic functionality and wood anatomy. *Sci. Total Environ.* 878, 163124 <https://doi.org/10.1016/j.scitotenv.2023.163124>.
- Gram, W.K., Sork, V.L., 2001. Association between environmental and genetic heterogeneity in forest tree populations. *Ecology* 82 (7), 2012–2021. [https://doi.org/10.1890/0012-9658\(2001\)082\[2012:ABEAGH\]2.0.CO;2](https://doi.org/10.1890/0012-9658(2001)082[2012:ABEAGH]2.0.CO;2).
- Granda, E., Camarero, J.J., Gimeno, T.E., Martínez-Fernández, J., Valladares, F., 2013. Intensity and timing of warming and drought differentially affect growth patterns of co-occurring Mediterranean tree species. *Eur. J. For. Res.* 132, 469–480. <https://doi.org/10.1007/s10342-013-0687-0>.
- Grossiord, C., Buckley, T.N., Cernusak, L.A., Novick, K.A., Poulter, B., Siegwolf, R.T., McDowell, N.G., 2020. Plant responses to rising vapor pressure deficit. *New Phytol.* 226 (6), 1550–1566. <https://doi.org/10.1111/nph.16485>.
- Guichoux, E., Lagache, L., Wagner, S., Léger, P., Petit, R.J., 2011. Two highly validated multiplexes (12-plex and 8-plex) for species delimitation and parentage analysis in oaks (*Quercus* spp.). *Mol. Ecol. Resour.* 11 (3), 578–585. <https://doi.org/10.1111/j.1755-0998.2011.02983.x>.
- Hackett-Pain, A., Bogdziewicz, M., 2021. Climate change and plant reproduction: trends and drivers of mast seeding change. *Philos. Trans. R. Soc. B* 376 (1839), 20200379. <https://doi.org/10.1098/rstb.2020.0379>.
- Harris, I., Osborn, T.J., Jones, P., Lister, D., 2020. Version 4 of the CRU TS monthly high-resolution gridded multivariate climate dataset. *Sci. Data* 7 (1), 109. <https://doi.org/10.1038/s41597-020-0453-3>.
- Hartmann, D.L., Tank, A.M.K., Rusticucci, M., Alexander, L.V., Brönnimann, S., Charabi, Y.A.R., Dentener, F.J., Dlugokencky, E.J., Easterling, D.R., Kaplan, A., et al., 2013. Observations: atmosphere and surface. In: *Climate Change 2013 The Physical Science Basis: Working Group I Contribution to the Fifth Assessment Report of the Intergovernmental Panel on Climate Change*, 2013. Cambridge University Press, Cambridge, UK. <https://doi.org/10.1017/CBO9781107415324.008>.
- Helle, G., Schleser, G.H., 2004a. Beyond CO₂-fixation by Rubisco—an interpretation of 13C/12C variations in tree rings from novel intra-seasonal studies on broad-leaf trees. *Plant Cell Environ.* 27 (3), 367–380. <https://doi.org/10.1111/j.0016-8025.2003.01159.x>.
- Helle, G., Schleser, G.H., 2004b. Interpreting climate proxies from tree-rings. In: *In The Climate in Historical Times: Towards a Synthesis of Holocene Proxy Data and Climate Models*. Springer Berlin Heidelberg, Berlin, Heidelberg, pp. 129–148.
- Hereñ, A.M., Kaye, M.W., Granda, E., Benavides, R., Lázaro-Nogal, A., Rubio-Casal, A.E., Yuste, J.C., 2018. Tree vigour influences secondary growth but not responsiveness to climatic variability in Holm oak. *Dendrochronologia* 49, 68–76. <https://doi.org/10.1016/j.dendro.2018.03.004>.
- Hereñ, J., Martínez-Vilalta, B.C., 2012. LópezGrowth patterns in relation to drought-induced mortality at two scots pine (*Pinus sylvestris* L.) sites in NE Iberian peninsula. *Trees* 26 (2), 621–630. <https://doi.org/10.1007/s00468-011-0628-9>.
- IPCC, 2022. In: Pörtner, H.-O., Roberts, D.C., Tignor, M., Poloczanska, E.S., Mintenbeck, K., Alegría, A., Craig, M., Langsdorf, S., Löschke, S., Möller, V., Okem, A., Rama, B. (Eds.), *Climate Change 2022: Impacts, Adaptation and Vulnerability*. Contribution of Working Group II to the Sixth Assessment Report of the Intergovernmental Panel on Climate Change. Cambridge University Press.
- Cambridge University Press, Cambridge, UK and New York, NY, USA. <https://doi.org/10.1017/9781009325844>, 3056 pp.
- Jäggi, M., Saurer, M., Fuhrer, J., Siegwolf, R., 2002. The relationship between the stable carbon isotope composition of needle bulk material, starch, and tree rings in *Picea abies*. *Oecologia* 131 (3), 325–332. <https://doi.org/10.1007/s00442-002-0881-0>.
- Joffre, R., Rambal, S., Ratte, J.P., 1999. The dehesa system of southern Spain and Portugal as a natural ecosystem mimic. *Agrofor. Syst.* 45, 57–79. <https://doi.org/10.1023/A:1006259402496>.
- Kamvar, Z.N., Tabima, J.F., Grünwald, N.J., 2014. Poppr: an R package for genetic analysis of populations with clonal, partially clonal, and/or sexual reproduction. *PeerJ* 2, e281. <https://doi.org/10.7717/peerj.281>.
- Keel, S.G., Siegwolf, R.T., Jäggi, M., Körner, C., 2007. Rapid mixing between old and new C pools in the canopy of mature forest trees. *Plant Cell Environ.* 30 (8), 963–972. <https://doi.org/10.1111/j.1365-3040.2007.01688.x>.
- Klein, T., Shpringer, I., Fikler, B., Elbaz, G., Cohen, S., Yakir, D., 2013. Relationships between stomatal regulation, water-use, and water-use efficiency of two coexisting key Mediterranean tree species. *For. Ecol. Manag.* 302, 34–42. <https://doi.org/10.1016/j.foreco.2013.03.044>.
- Kremer, A., Le Corre, V., Petit, R.J., Ducousso, A., 2010. Historical and contemporary dynamics of adaptive differentiation in European oaks. In: DeWoody, J.A., Bickham, J.W., Michler, C.H., Nichols, K.M., Rhodes, O.E., Woeste, K.E. (Eds.), *Molecular Approaches in Natural Resource Conservation and Management*. Academic Press, New York, NY, pp. 101–122.
- Le Provost, G., Gerardin, T., Plomion, C., Brendel, O., 2022. Molecular plasticity to soil water deficit differs between sessile oak (*Quercus Petraea* (Matt.) Liebl.) high-and low-water use efficiency genotypes. *Tree Physiol.* 42 (12), 2546–2562. <https://doi.org/10.1093/treephys/tpac087>.
- Le Roncé, I., Gavinet, J., Ourcival, J.M., Mouillot, F., Chuine, I., Limousin, J.M., 2021. Holm oak fecundity does not acclimate to a drier world. *New Phytol.* 231 (2), 631–645. <https://doi.org/10.1111/nph.17412>.
- Lebourgeois, F., Mérian, P., Courdier, F., Ladier, J., Dreyfus, P., 2012. Instability of climate signal in tree-ring width in Mediterranean mountains: a multi-species analysis. *Trees* 26, 715–729. <https://doi.org/10.1007/s00468-011-0638-7>.
- Leite, C., Oliveira, V., Lauw, A., Pereira, H., 2019. Cork rings suggest how to manage *Quercus suber* to mitigate the effects of climate changes. *Agric. For. Meteorol.* 266, 12–19. <https://doi.org/10.1016/j.agrformet.2018.11.032>.
- Limousin, J.M., Misson, L., Lavoie, A.V., Martin, N.K., Rambal, S., 2010. Do photosynthetic limitations of evergreen *Quercus ilex* leaves change with long-term increased drought severity? *Plant Cell Environ.* 33 (5), 863–875. <https://doi.org/10.1111/j.1365-3040.2009.02112.x>.
- Limousin, J.M., Roussel, A., Rodríguez-Calcerrada, J., Torres-Ruiz, J.M., Moreno, M., García de Jalón, L., Martín-StPaul, N., 2022. Drought acclimation of *Quercus ilex* leaves improves tolerance to moderate drought but not resistance to severe water stress. *Plant Cell Environ.* 45 (7), 1967–1984. <https://doi.org/10.1111/pce.14326>.
- Linaldeddu, B.T., Scanu, B., Maddau, L., Franceschini, A., 2014. *Diplodia corticola* and *Phytophthora cinnamomi*: the main pathogens involved in holm oak decline on Caprera Island (Italy). *For. Pathol.* 44 (3), 191–200. <https://doi.org/10.1111/efp.12081>.
- Livingston, N.J., Whitehead, D., Kelliher, F.M., Wang, Y.P., Grace, J.C., Walcroft, A.S., Millard, P., 1998. Nitrogen allocation and carbon isotope fractionation in relation to intercepted radiation and position in a young *Pinus radiata* D. Don tree. *Plant Cell Environ.* 21 (8), 795–803. <https://doi.org/10.1046/j.1365-3040.1998.00314.x>.
- Lloret, D., Siscart, C., 2004. Dalmases canopy recovery after drought dieback in holm-oak Mediterranean forests of Catalonia (NE Spain). *Glob. Chang. Biol.* 10, 2092–2099. <https://doi.org/10.1111/j.1365-2486.2004.00870.x>.
- Lloret, F., García, C., 2016. Inbreeding and neighbouring vegetation drive drought-induced die-off within juniper populations. *Funct. Ecol.* 30 (10), 1696–1704. <https://doi.org/10.1111/1365-2435.12655>.
- Lloret, F., Keeling, E.G., Sala, A., 2011. Components of tree resilience: effects of successive low-growth episodes in old ponderosa pine forests. *Oikos* 120 (12), 1909–1920. <https://doi.org/10.1111/j.1600-0706.2011.19372.x>.
- Lobo, A., Torres-Ruiz, J.M., Burlett, R., Lemaire, C., Parise, C., Francioni, C., Delzon, S., 2018. Assessing inter- and intraspecific variability of xylem vulnerability to embolism in oaks. *For. Ecol. Manag.* 424, 53–61. <https://doi.org/10.1016/j.foreco.2018.04.031>.
- López, R., Cano, F.J., Rodríguez-Calcerrada, J., Sangüesa-Barreda, G., Gazol, A., Camarero, J.J., Gil, L., 2021. Tree-ring density and carbon isotope composition are early-warning signals of drought-induced mortality in the drought tolerant Canary Island pine. *Agric. For. Meteorol.* 310, 108634 <https://doi.org/10.1016/j.agrformet.2021.108634>.
- Madritsch, S., Wischnitzki, E., Kotrade, P., Ashoub, A., Burg, A., Fluch, S., Sehr, E.M., 2019. Elucidating drought stress tolerance in European oaks through cross-species transcriptomics. *G3: Genes, Genomes, Genet.* 9 (10), 3181–3199. <https://doi.org/10.1534/g3.119.400456>.
- Maldonado-Alconada, A.M., Castillejo, M.A., Rey, M.D., Labella-Ortega, M., Tienda-Parrilla, M., Hernández-Lao, T., Jorrión-Novo, J.V., 2022. Multiomics molecular research into the recalcitrant and orphan *Quercus ilex* tree species: why, what for, and how. *Int. J. Mol. Sci.* 23 (17), 9980. <https://doi.org/10.3390/ijms23179980>.
- Manetti, M.C., Bartolucci, S., Bertini, G., Piusi, P., Sani, L., 2009. Dinamiche naturali in formazioni forestali a prevalenza di leccio nel Parco Regionale della Maremma. *Forest@* 6, 186–198. Retrieved from <http://www.sisef.it/forest@doi:10.3832/efor0580-006>.
- Marguerit, E., Bouffier, L., Chancerel, E., Costa, P., Lagane, F., Guehl, J.M., Brendel, O., 2014. The genetics of water-use efficiency and its relation to growth in maritime pine. *J. Exp. Bot.* 65 (17), 4757–4768. <https://doi.org/10.1093/jxb/eru226>.

- Mariotti, Y., Pan, N., Zeng, A., 2015. Alessandri Long-term climate change in the Mediterranean region in the midst of decadal variability. *Clim. Dyn.* 44, 1437–1456. <https://doi.org/10.1007/s00382-015-2487-3>.
- Martínez-villalta, J., López, B.C., Adell, N., Badiella, L., Ninyerola, M., 2008. Twentieth century increase of Scots pine radial growth in NE Spain shows strong climate interactions. *Glob. Chang. Biol.* 14 (12), 2868–2881. <https://doi.org/10.1111/j.1365-2486.2008.01685.x>.
- McCarroll, D., Loader, N.J., 2004. Stable isotopes in tree rings. *Quat. Sci. Rev.* 23 (7–8), 771–801.
- McDowell, N., Pockman, W.T., Allen, C.D., Breshears, D.D., Cobb, N., Kolb, T., Yepez, E. A., 2008. Mechanisms of plant survival and mortality during drought: why do some plants survive while others succumb to drought? *New Phytol.* 178 (4), 719–739. <https://doi.org/10.1111/j.1469-8137.2008.02436.x>.
- McDowell, N.G., Beerling, D.J., Breshears, D.D., Fisher, R.A., Raffa, K.F., Stitt, M., 2011. The interdependence of mechanisms underlying climate-driven vegetation mortality. *Trends Ecol. Evol.* 26 (10), 523–532. <https://doi.org/10.1016/j.tree.2011.06.003>.
- McDowell, N.G., Allen, C.D., Anderson-Teixeira, K., Aukema, B.H., Bond-Lamberty, B., Chini, L., Xu, C., 2020. Pervasive shifts in forest dynamics in a changing world. *Science* 368 (6494), eaaz9463. <https://doi.org/10.1126/science.aaz9463>.
- Montserrat-Martí, G., Camarero, J.J., Palacio, S., Pérez-Rontomé, C., Milla, R., Albuixech, J., Maestro, M., 2009. Summer-drought constrains the phenology and growth of two coexisting Mediterranean oaks with contrasting leaf habit: implications for their persistence and reproduction. *Trees* 23, 787–799. <https://doi.org/10.1007/s00468-009-0320-5>.
- Natalini, F., Alejano, R., Vázquez-Piqué, J., Cañellas, I., Gea-Izquierdo, G., 2016. The role of climate change in the widespread mortality of holm oak in open woodlands of Southwestern Spain. *Dendrochronologia* 38, 51–60. <https://doi.org/10.1016/j.dendro.2016.03.003>.
- Nijland, W., Jansma, E., Addink, E.A., Domínguez Delmás, M., De Jong, S.M., 2011. Relating ring width of Mediterranean evergreen species to seasonal and annual variations of precipitation and temperature. *Biogeosciences* 8 (5), 1141–1152. <https://doi.org/10.5194/bg-8-1141-2011>.
- Ortego, J., Bonal, R., Muñoz, A., 2010. Genetic Consequences of habitat fragmentation in long-lived tree species: the case of the Mediterranean holm oak (*Quercus ilex*, L.). *J. Hered.* 101 (6), 717–726. <https://doi.org/10.1093/jhered/esq081>.
- Park Williams, A., Allen, C.D., Macalady, A.K., Griffin, D., Woodhouse, C.A., Meko, D.M., McDowell, N.G., 2013. Temperature as a potent driver of regional forest drought stress and tree mortality. *Nat. Clim. Chang.* 3 (3), 292–297. <https://doi.org/10.7916/d8-b9ec-8z87>.
- Pasho, E., Camarero, J.J., de Luis, M., Vicente-Serrano, S.M., 2012. Factors driving growth responses to drought in Mediterranean forests. *Eur. J. For. Res.* 131 (6), 1797–1807. <https://doi.org/10.1007/s10342-012-0633-6>.
- Pasquini, D., Gori, A., Pollastrini, M., Alderotti, F., Centritto, M., Ferrini, F., Brunetti, C., 2023. Effects of drought-induced holm oak dieback on BVOCs emissions in a Mediterranean forest. *Sci. Total Environ.* 857, 159635. <https://doi.org/10.1016/j.scitotenv.2022.159635>.
- Peakall, R., Smouse, R.P.P., 2012. GenAlEx 6.5: genetic analysis in Excel. Population genetic software for teaching and research—an update. *Bioinformatics* 28 (19), 2537–2539. <https://doi.org/10.1111/j.1471-8286.2005.01155.x>.
- Peltier, D.M., Ogle, K., 2020. Tree growth sensitivity to climate is temporally variable. *Ecol. Lett.* 23 (11), 1561–1572. <https://doi.org/10.1111/ele.13575>.
- Peñuelas, J., Filella, I., Lloret, F., Piñol, J., Siscart, D., 2000. Effects of a severe drought on water and nitrogen use by *Quercus ilex* and *Phillyrea latifolia*. *Biol. Plant.* 43, 47–53. <https://doi.org/10.1023/A:1026546828466>.
- Petrucchio, L., Nardini, A., Von Arx, G., Saurer, M., Cherubini, P., 2017. Isotope signals and anatomical features in tree rings suggest a role for hydraulic strategies in diffuse drought-induced die-back of *Pinus nigra*. *Tree Physiol.* 37 (4), 523–535. <https://doi.org/10.1093/treephys/tpx031>.
- Pollastrini, M., Puletti, N., Selvi, F., Iacopetti, G., Bussotti, F., 2019. Widespread crown defoliation after a drought and heat wave in the forests of Tuscany (central Italy) and their recovery—a case study from summer 2017. *Front. For. Glob. Change* 2, 74. <https://doi.org/10.3389/ffgc.2019.00074>.
- Prieto, P., Peñuelas, J., Llusià, J., Asensio, D., Estiarte, M., 2009. Effects of long-term experimental night-time warming and drought on photosynthesis, Fv/Fm and stomatal conductance in the dominant species of a Mediterranean shrubland. *Acta Physiol. Plant.* 31, 729–739. <https://doi.org/10.1007/s11738-009-0285-4>.
- Pritchard, J.K., Stephens, M., Donnelly, P., 2000. Inference of population structure using multilocus genotype data. *Genetics* 155 (2), 945–959. <https://doi.org/10.1093/genetics/155.2.945>.
- Puchi, P.F., Camarero, J.J., Battipaglia, G., Carrer, M., 2021. Retrospective analysis of wood anatomical traits and tree-ring isotopes suggests site-specific mechanisms triggering *Araucaria araucana* drought-induced dieback. *Glob. Chang. Biol.* 27 (24), 6394–6408. <https://doi.org/10.1111/gcb.15881>.
- Puletti, N., Mattioli, W., Bussotti, F., Pollastrini, M., 2019. Monitoring the effects of extreme drought events on forest health by Sentinel-2 imagery. *J. Appl. Remote. Sens.* 13 (2), 1–8. <https://doi.org/10.1117/1.JRS.13.020501>.
- Ramírez-Valiente, J.A., Lorenzo, Z., Soto, A., Valladares, F., Gil, L., Aranda, I., 2009. Elucidating the role of genetic drift and natural selection in cork oak differentiation regarding drought tolerance. *Mol. Ecol.* 18 (18), 3803–3815. <https://doi.org/10.1111/j.1365-294X.2009.04317.x>.
- Rinn, F., 2016. TSAP-Win: Time Series Analysis and Presentation for Dendrochronology and Related Applications: Version 0.55 User Reference. RINNTECH, Heidelberg, Germany.
- Ripullone, F., Camarero, J.J., Colangelo, M., Voltas, J., 2020. Variation in the access to deep soil water pools explains tree-to-tree differences in drought-triggered dieback of Mediterranean oaks. *Tree Physiol.* 40 (5), 591–604. <https://doi.org/10.1093/treephys/tpaa026>.
- Rita, A., Camarero, J.J., Nolè, A., Borghetti, M., Brunetti, M., Pergola, N., Ripullone, F., 2020. The impact of drought spells on forests depends on site conditions: the case of 2017 summer heat wave in southern Europe. *Glob. Chang. Biol.* 26 (2), 851–863. <https://doi.org/10.1111/gcb.14825>.
- Rodríguez-Calcerrada, J., Li, M., López, R., Cano, F.J., Oleksyn, J., Atkin, O.K., Gil, L., 2017. Drought-induced shoot dieback starts with massive root xylem embolism and variable depletion of non-structural carbohydrates in seedlings of two tree species. *New Phytol.* 213 (2), 597–610. <https://doi.org/10.1111/nph.14150>.
- Roussel, M., Dreyer, E., Montpied, P., Le-Provost, G., Guehl, J.M., Brendel, O., 2009. The diversity of ^{13}C isotope discrimination in a *Quercus robur* full-sib family is associated with differences in intrinsic water use efficiency, transpiration efficiency, and stomatal conductance. *J. Exp. Bot.* 60 (8), 2419–2431.
- Ruiz-Gómez, F.J., Pérez-de-Luque, A., Navarro-Cerrillo, R.M., 2019. The involvement of Phytophthora root rot and drought stress in holm oak decline: from ecophysiology to microbiome influence. *Curr. For. Rep.* 5, 251–266. <https://doi.org/10.1093/jxb/erf100>.
- San-Eufasio, B., Sánchez-Lucas, R., López-Hidalgo, C., Guerrero-Sánchez, V.M., Castillejo, M.Á., Maldonado-Alconada, A.M., Rey, M.D., 2020. Responses and differences in tolerance to water shortage under climatic dryness conditions in seedlings from *Quercus* spp. and Andalusian *Q. ilex* populations. *Forests* 11 (6), 707. <https://doi.org/10.3390/f11060707>.
- San-Eufasio, B., Castillejo, M.Á., Labella-Ortega, M., Ruiz-Gómez, F.J., Navarro-Cerrillo, R.M., Tienda-Parrilla, M., Rey, M.D., 2021. Effect and response of *Quercus ilex* subsp. *ballota* [Desf.] Samp. seedlings from three contrasting Andalusian populations to individual and combined *Phytophthora cinnamomi* and drought stresses. *Front. Plant Sci.* 12, 722802. <https://doi.org/10.3389/fpls.2021.722802>.
- Santini, F., Shestakova, T.A., Dashevskaya, S., Notivol, E., Voltas, J., 2020. Dendroecological and genetic insights for future management of an old-planted forest of the endangered Mediterranean fir *Abies pinsapo*. *Dendrochronologia* 63, 125754. <https://doi.org/10.1016/j.dendro.2020.125754>.
- Saurer, M., Sahlstedt, E., Rinne-Garmston, K.T., Lehmann, M.M., Oettli, M., Gessler, A., Treydte, K., 2022. High-resolution isotope analysis of tree rings. *Tree Physiol.* <https://doi.org/10.1093/treephys/tpac141>.
- Savi, T., Casolo, V., Dal Borgo, A., Rosner, S., Torboli, V., Stenni, B., Nardini, A., 2019. Drought-induced dieback of *Pinus nigra*: a tale of hydraulic failure and carbon starvation. *Conserv. Physiol.* 7 (1), coz012. <https://doi.org/10.1093/conphys/coz012>.
- Scheidegger, Y., Saurer, M., Bahn, M., Siegwolf, R., 2000. Linking stable oxygen and carbon isotopes with stomatal conductance and photosynthetic capacity: a conceptual model. *Oecologia* 125, 350–357. <https://doi.org/10.1007/s004420000466>.
- Schwärzel, K., Zhang, L., Montanarella, L., Wang, Y., Sun, G., 2020. How afforestation affects the water cycle in drylands: a process-based comparative analysis. *Glob. Chang. Biol.* 26 (2), 944–959. <https://doi.org/10.1111/gcb.14875>.
- Shamari, A.R., Mehrabi, A.A., Maleki, A., Rostami, A., 2018. Association analysis of tolerance to dieback phenomena and trunk form using ISSR markers in *Quercus brantii*. *Cell. Mol. Biol.* 64 (13), 116–124. <https://doi.org/10.14715/cmb/2018.64.13.22>.
- Shestakova, T.A., Martínez-Sancho, E., 2021. Stories hidden in tree rings: a review on the application of stable carbon isotopes to dendrosciences. *Dendrochronologia* 65, 125789. <https://doi.org/10.1016/j.dendro.2020.125789>.
- Shestakova, T.A., Aguilera, M., Ferrio, J.P., Gutiérrez, E., Voltas, J., 2014. Unravelling spatiotemporal tree-ring signals in Mediterranean oaks: a variance-covariance modelling approach of carbon and oxygen isotope ratios. *Tree Physiol.* 34 (8), 819–838. <https://doi.org/10.1093/treephys/tpu037>.
- Sillo, F., Giordano, L., Zampieri, E., Lione, G., De Cesare, S., Gonthier, P., 2017. HRM analysis provides insights on the reproduction mode and the population structure of *Gnomoniopsis castaneae* in Europe. *Plant Pathol.* 66 (2), 293–303. <https://doi.org/10.1111/ppa.12571>.
- Valbuena-Carabana, M., González-Martínez, S.C., Gil, L., 2008. Coppice forests and genetic diversity: a case study in *Quercus pyrenaica* Willd. from Central Spain. *For. Ecol. Manag.* 254 (2), 225–232. <https://doi.org/10.1016/j.foreco.2007.08.001>.
- Venegas-González, Alejandro, Gibson-Capinero, Stephanie, Anholetto-Junior, Claudio, Mathiasen, Paula, Premoli, Andrea Cecilia, Fresia, Pablo, 2022. Tree-ring analysis and genetic associations help to understand drought sensitivity in the Chilean Endemic Forest of *Nothofagus macrocarpa*. *Front. For. Glob. Change* 5, 2. <https://doi.org/10.3389/ffgc.2022.762347>.
- Vicente-Serrano, S.M., Beguería, S., López-Moreno, J.I., 2010. A multiscale drought index sensitive to global warming: the standardized precipitation evapotranspiration index. *J. Clim.* 23 (7) <https://doi.org/10.1175/2009JCLI2909.1>.
- Voltas, J., Camarero, J.J., Carulla, D., Aguilera, M., Ortiz, A., Ferrio, J.P., 2013. A retrospective, dual-isotope approach reveals individual predispositions to winter-drought induced tree dieback in the southernmost distribution limit of Scots pine. *Plant Cell Environ.* 36 (8), 1435–1448. <https://doi.org/10.1111/pce.12072>.
- Weigt, R.B., Bräunlich, S., Zimmermann, L., Saurer, M., Grams, T.E., Dietrich, H.P., Nikolova, P.S., 2015. Comparison of $\delta^{18}\text{O}$ and $\delta^{13}\text{C}$ values between tree-ring whole wood and cellulose in five species growing under two different site conditions. *Rapid Commun. Mass Spectrom.* 29 (23), 2233–2244. <https://doi.org/10.1002/rcm.7388>.
- Wigley, T.M.L., Briffa, K.R., Jones, P.D., 1984. On the average value of correlated time series, with applications in dendroclimatology and hydrometeorology. *J. Clim. Appl. Meteorol.* 23, 201–213. [https://doi.org/10.1175/1520-0450\(1984\)023<0201:OTAVOC>2.0.CO;2](https://doi.org/10.1175/1520-0450(1984)023<0201:OTAVOC>2.0.CO;2).
- Yakir, D., Israeli, Y., 1995. Reduced solar irradiance effects on net primary productivity (NPP) and the $\delta^{13}\text{C}$ and $\delta^{18}\text{O}$ values in plantations of *Musa* sp., *Musaceae*. *Geochim.*

- Cosmochim. Acta 59, 2149–2151. [https://doi.org/10.1016/S0016-7037\(99\)80010-6](https://doi.org/10.1016/S0016-7037(99)80010-6).
- Zadworny, et al., 2019. Regeneration origin affects radial growth patterns preceding oak decline and death—insights from tree-ring $\delta^{13}\text{C}$ and $\delta^{18}\text{O}$. *Agric. For. Meteorol.* 278, 107685 <https://doi.org/10.1016/j.agrformet.2019.107685>.
- Zalloni, E., Battipaglia, G., Cherubini, P., De Micco, V., 2018. Site conditions influence the climate signal of intra-annual density fluctuations in tree rings of *Q. ilex* L. *Ann. For. Sci.* 75 (3), 1–12. <https://doi.org/10.1007/s13595-018-0748-0>.